ESC European Society of Cardiology

Cardiovascular Research (2023) **119**, 982–997
https://doi.org/10.1093/cvr/cvad005

Dietary essential amino acids for the treatment of heart failure with reduced ejection fraction

Maurizio Ragni[1], Carolina Magdalen Greco[2,3], Arianna Felicetta [2], Shuxun Vincent Ren[4], Paolo Kunderfranco[2], Chiara Ruocco[1], Pierluigi Carullo [2,5], Veronica Larcher[2], Laura Tedesco[1], Ilenia Severi[6], Antonio Giordano[6], Saverio Cinti[6], Alessandra Valerio[7], Haipeng Sun[4†], Yibin Wang[4], Chen Gao[4], Gianluigi Condorelli[2,3,4], and Enzo Nisoli [1]*

[1]Center for Study and Research on Obesity, Department of Medical Biotechnology and Translational Medicine, University of Milan, Via Vanvitelli 32, Milan 20129, Italy; [2]Department of Cardiovascular Medicine, Humanitas Research Hospital, Via Manzoni 56, 20089 Rozzano (Milan), Italy; [3]Department of Biomedical Sciences, Humanitas University, Via Rita Levi Montalcini 4, 20090 Pieve Emanuele (Milan), Italy; [4]Departments of Anesthesiology, Medicine and Physiology, David Geffen School of Medicine at University of California, Los Angeles, 90095 CA, United States; [5]National Research Council of Italy, Institute of Genetics and Biomedical Research, Milan 20090, Italy; [6]Department of Experimental and Clinical Medicine, Marche Polytechnic University, Ancona 60126, Italy; and [7]Department of Molecular and Translational Medicine, University of Brescia, Brescia 25123, Italy

Received 24 June 2022; revised 5 November 2022; editorial decision 11 November 2022; online publish-ahead-of-print 10 January 2023

Aims

Heart failure with reduced ejection fraction (HFrEF) is a leading cause of mortality worldwide, requiring novel therapeutic and lifestyle interventions. Metabolic alterations and energy production deficit are hallmarks and thereby promising therapeutic targets for this complex clinical syndrome. We aim to study the molecular mechanisms and effects on cardiac function in rodents with HFrEF of a designer diet in which free essential amino acids—in specifically designed percentages—substituted for protein.

Methods and results

Wild-type mice were subjected to transverse aortic constriction (TAC) to induce left ventricle (LV) pressure overload or sham surgery. Whole-body glucose homeostasis was studied with glucose tolerance test, while myocardial dysfunction and fibrosis were measured with echocardiogram and histological analysis. Mitochondrial bioenergetics and morphology were investigated with oxygen consumption rate measurement and electron microscopy evaluation. Circulating and cardiac non-targeted metabolite profiles were analyzed by ultrahigh performance liquid chromatography-tandem mass spectroscopy, while RNA-sequencing was used to identify signalling pathways mainly affected. The amino acid-substituted diet shows remarkable preventive and therapeutic effects. This dietary approach corrects the whole-body glucose metabolism and restores the unbalanced metabolic substrate usage—by improving mitochondrial fuel oxidation—in the failing heart. In particular, biochemical, molecular, and genetic approaches suggest that renormalization of branched-chain amino acid oxidation in cardiac tissue, which is suppressed in HFrEF, plays a relevant role. Beyond the changes of systemic metabolism, cell-autonomous processes may explain at least in part the diet's cardioprotective impact.

Conclusion

Collectively, these results suggest that manipulation of dietary amino acids, and especially essential amino acids, is a potential adjuvant therapeutic strategy to treat systolic dysfunction and HFrEF in humans.

* Corresponding author. Tel: +39 (02) 50316956, Fax: +39 02 50317118, E-mail: enzo.nisoli@unimi.it
† Present address: Department of Pathophysiology, Hongqiao International Institute of Medicine, Tongren Hospital, Key Laboratory of Cell Differentiation and Apoptosis of Chinese Ministry of Education, Shanghai Jiao Tong University, School of Medicine, Shanghai, 200240, China.

Graphical Abstract

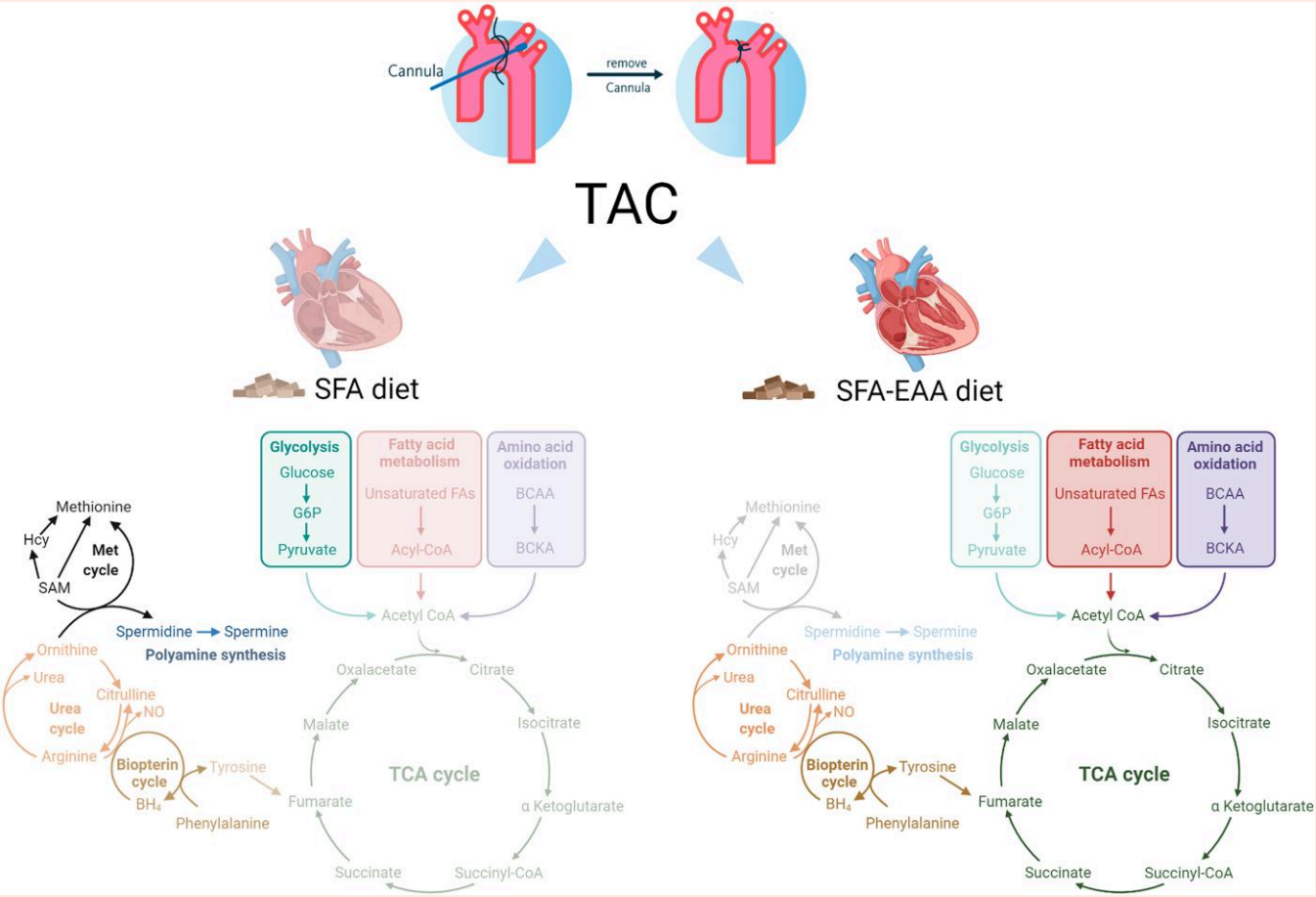

Keywords Amino acids • Heart failure • Mitochondrial function • Nutrition • Transcriptomic reprogramming

1. Introduction

Heart failure (HF) is a major cause of hospitalization and mortality, imposing substantial public health and economic burden worldwide.[1,2] The use of β-adrenergic receptor and renin–angiotensin antagonists, aldosterone receptor antagonists, and the recent angiotensin receptor neprilysin inhibitor has improved morbidity and mortality rates. Sodium-glucose cotransporter 2 inhibitors have added novel cardioprotective therapeutic approaches, practical to ameliorate cardiac dysfunction and increase exercise capacity in patients with HF with reduced ejection fraction (HFrEF), and to reduce at least hospitalization in patients with HF with preserved ejection fraction (HFpEF), for whom there are so far no evidence-based therapies.[3] However, both HFrEF and HFpEF patients still have poor long-term outcomes,[4] highlighting the need for novel therapeutic and lifestyle interventions.

HFrEF is associated with an imbalance of energy metabolism, characterized by perturbations in mitochondrial function, redox reactions,[5] adenosine triphosphate synthesis,[6] and substrate utilization (*i.e.* reduced fatty acid and pyruvate oxidation and increased glucose utilization).[7,8] More recent studies have identified the critical role of amino acid metabolism perturbation in the pathogenesis of HFrEF.[9] They suggest how restoring the mitochondrial branched-chain amino acid (BCAA) oxidation—characteristically damaged in failing heart—improves cardiac metabolic flexibility and alleviates systolic dysfunction in HFrEF.[10]

Several dietary interventions have been proposed as a valuable strategy to improve whole-body and cardiac energy metabolism and treat clinical conditions caused by impaired energy production. In contrast, no data on diet ability to improve BCAA oxidation have been reported yet. Supplementation of essential amino acids (EAAs) is beneficial for energy disorders such as sarcopenia, liver and kidney diseases, obesity, and type 2 diabetes.[11,12] Additionally, we previously found that the EAA supplementation extends survival in mice, mainly by promoting mitochondrial biogenesis, redox balance, and metabolic fitness in muscle and cardiac tissue.[13] Thus, it is plausible that specific nutritional approaches might advantage the HFrEF patients at least at the energy production level.[14,15]

Driven by this speculation, we examined whether consumption of an EAA-enriched diet attenuated systolic dysfunction in transverse aortic constriction (TAC)-induced left ventricle (LV) pressure overload, a mouse model of HFrEF. Here, we show that a customized diet, in which a precise formula of EAAs substitutes for protein content—without changing calorie amount and macronutrient percentage—exerts remarkable preventive and therapeutic anti-HFrEF effects in mice. These effects are partially mediated through improved energy metabolism, promoting myocardial bioenergetics, efficient substrate utilization, and reduced fibrosis in the heart. These results suggest a rationale for investigating the effect of our amino acid-substituted diet in humans with HFrEF.

2. Methods

2.1 Animal models, diets, and ethical considerations

All procedures involving animal use were conducted in accordance with the European Community Guidelines (Directive 2010/63/EU) and those of the Italian Ministry of Health (Legislative Decree No. 26/2014), complied with the National Animal Protection Guidelines, and were approved by the Institutional Animal Ethical Committee. Experiments with 2C-type serine-threonine protein phosphatase knockout mice ($PP2Cm^{-/-}$) were approved by UCLA IACUC in compliance of the US regulations and guidelines. Mice were housed in a temperature and humidity controlled facility with 12 h light/dark cycle and ad libitum access to food and water. Male C57BL/6N mice (8-weeks-old), from Charles River (Calco, Italy) or $PP2Cm^{-/-}$ mice[16] were weight-matched and fed *ad libitum* for different periods of time with normal chow diet (CD: V1534-300, Ssniff Spezialdiäten GmbH, Soest, Germany). Mice were then fed with the following experimental diets before (preventive protocol) or after (therapeutic protocol) surgical pressure overload induction (see also the Results section, *Figure 1A*, and Supplementary material online, *Figure S3A* for explanations): control SFA diet: (20% Kcal from protein—namely casein, 70% from carbohydrate, and 10 from % fat, half of which was lard (D12450H). SFA-EAA diet: isocaloric, isolipidic, and isonitrogenous with SFA diet except for casein content, which was almost entirely (93.5%) replaced by a defined mixture of free EAAs (D14032501). Control SFA-CAA diet: isocaloric, isolipidic, and isonitrogenous with SFA in which casein was substituted with free amino acids designed on the amino acid profile of casein (A17092801) (see Supplementary material online, *Table S1*). All diets were from Research Diets Inc. (Brogaarden, Gentofte, Denmark). Body weight and food intake were recorded twice a week in mice housed individually. Mice used have a C57BL/6N background, that does not exhibit defects of insulin release and mitochondrial dysfunction relative to C57BL/6J mice.[17] At the end of the experimental procedures, euthanasia was performed by cervical dislocation while the mice were under a surgical plane of anaesthesia; tissue samples for molecular analysis were snap-frozen in liquid nitrogen and prepared as described below.

2.2 Transverse aortic constriction

Mice were anaesthetized with a single intraperitoneal injection of a mixture of ketamine (100 mg/kg), xylazine (5 mg/kg), and morphine (2.5 mg/kg), in accordance with the European Community Guidelines (see above). Anaesthetized mice were closely monitored during the procedure to assure that they were maintained in the proper anaesthetic plane. In particular, the anaesthetic efficacy was assessed by pinching the tail of the animal while monitoring body temperature and respiratory rate. Any reaction of the animal, hypothermia or increase in respiratory rate indicated that anaesthesia was too light and that additional anaesthetic should be given. TAC surgery was adapted from Rockman et al.[18] Briefly, anaesthetized mice were placed in a supine position, the chest was shaved using a chemical hair remover, and the aortic arch was exposed through the first intercostal space. A 8–0 Prolene suture was passed between the truncus anonymous and the left carotid artery, a blunted 27-gauge needle was placed against the aorta and the knot tightened along with the needle and secured with a second knot. The needle was removed to create a lumen with a fixed stenotic diameter. The chest cavity was then closed with a 6–0 silk suture. A separate group of mice underwent the same surgical procedure but without any tightening of the knot (sham group). The pressure load caused by the knot was verified through the measurement of the pressure gradient across the aortic constriction with echocardiography. The mean pressure gradient (PG) in TAC mice was made to be ~70 mmHg in order to induce a rapid deterioration of heart function. PG was not significantly different between TAC animals fed with SFA or SFA-EAA diets (74 ± 10.1 mmHg and 78 ± 9.7 mmHg in TAC SFA and TAC SFA-EAA, respectively) ($P = 0.35$ with an unpaired Student's *t*-test).

2.3 Echocardiography

Echocardiography was performed on a Vevo 2100 (VisualSonics) system equipped with an MS550S probe 'high frame' scan head. Anaesthesia was induced with 3% isoflurane and maintained with a flow 1.0% isoflurane during constant monitoring of temperature, respiration rate, and ECG while maintaining heart rate at 450–550 beats per min. Two-dimensional cine loops with frame rates of 200 frames per second in long- and short-axis views of the LVs were recorded. End-diastolic (d) and end-systolic (s) intraventricular septum (IVSTd, IVSTs), posterior wall thickness (PWTd, PWTs) and LV internal diameters (LVEDd, LVEDs) were measured. Percentage fractional shortening (% FS) and relative ejection fraction (% EF) were calculated using standard formulas: $\%\ FS = [(LVEDd - LVEDs)/LVEDd] \times 100$; $\%\ EF = [(LVEDV - LVESV)/LVEDV] \times 100$.

2.4 Immunoblot analysis

Protein extracts were obtained from tissues using T-PER Mammalian Protein Extraction Reagent (Pierce, Euroclone, Milan, Italy) as indicated by the manufacturer, in the presence of a cocktail of protease and phosphatase inhibitors (Sigma-Aldrich, Milan, Italy). Concentration of proteins was determined using BCA Protein Assay Reagent (Euroclone, Milan, Italy). Fifteen to twenty micrograms of proteins were separated on a 4–12% SDS-PAGE gel and transferred to PVDF membranes (Bio-Rad Laboratories, Milan, Italy). Membranes where then incubated with the primary antibodies and detection was performed using horseradish peroxidase conjugated anti-rabbit or anti-mouse immunoglobulin for 1 h at room temperature. Image acquisition was performed using SuperSignal Substrate (Pierce) and analyzed using ImageQuant TL software. For detection of phosphoproteins, filters were stripped with Strip Blot (Euroclone, Milan, Italy) and further used for the visualization of total proteins. Primary antibodies (each at 1:1 000 dilution) are listed in Supplementary material online, *Table S2*.

2.5 Insulin receptor substrate pan-tyrosine phosphorylation

Pan-tyrosine phosphorylation of insulin receptor substrate (IRS) was determined using PathScan Sandwich ELISA kits (Cell Signaling Technology) according to the manufacturer's instruction.

2.6 Histology

Hearts were fixed in 10% buffered formalin and embedded in paraffin. Histology and immunostaining were performed on 5 μm-thick paraffin sections. Fibrosis was quantified using the Trichrome Stain (Masson) Kit (Sigma, HT15). Quantification of the fibrotic area was performed with ImageJ. After deparaffinization, tissue sections were incubated with an anti-wheat germ agglutinin (anti-WGA, Sigma-Aldrich) antibody, which marks fibrotic tissue in comparable quality as the established picrosirius red (SR) staining. Images were acquired with an SP8II Imaging system, and the cardiomyocyte cross-area sectional area was quantified with ImageJ.

2.7 Electron microscopy

Hearts from perfused mice were further fixed in 2.5% glutaraldehyde and 2% formaldehyde in 0.1 M phosphate buffer over night at 4°C, post-fixed in 1% osmium tetroxide, dehydrated in acetone, and embedded in epoxy resin (all from Electron Microscopy Science, Società Italiana Chimici, Rome, Italy). Semi-thin sections (2 μm) were stained with toluidine blue. Thin sections obtained with an MT-X ultratome (RCM, Tucson, AZ, USA) were mounted on copper grids, stained with lead citrate and examined with a EM208 transmission electron microscope (Philips, Eindhoven, The Netherlands). Mean mitochondrial area, mitochondria density (number of mitochondria/area expressed in μm^2, normalyzed in 10 μm^2) and number of mitochondria cristae (number of cristae/mitochondria area, normalized in 1 μm^2) were determined by ImageJ.

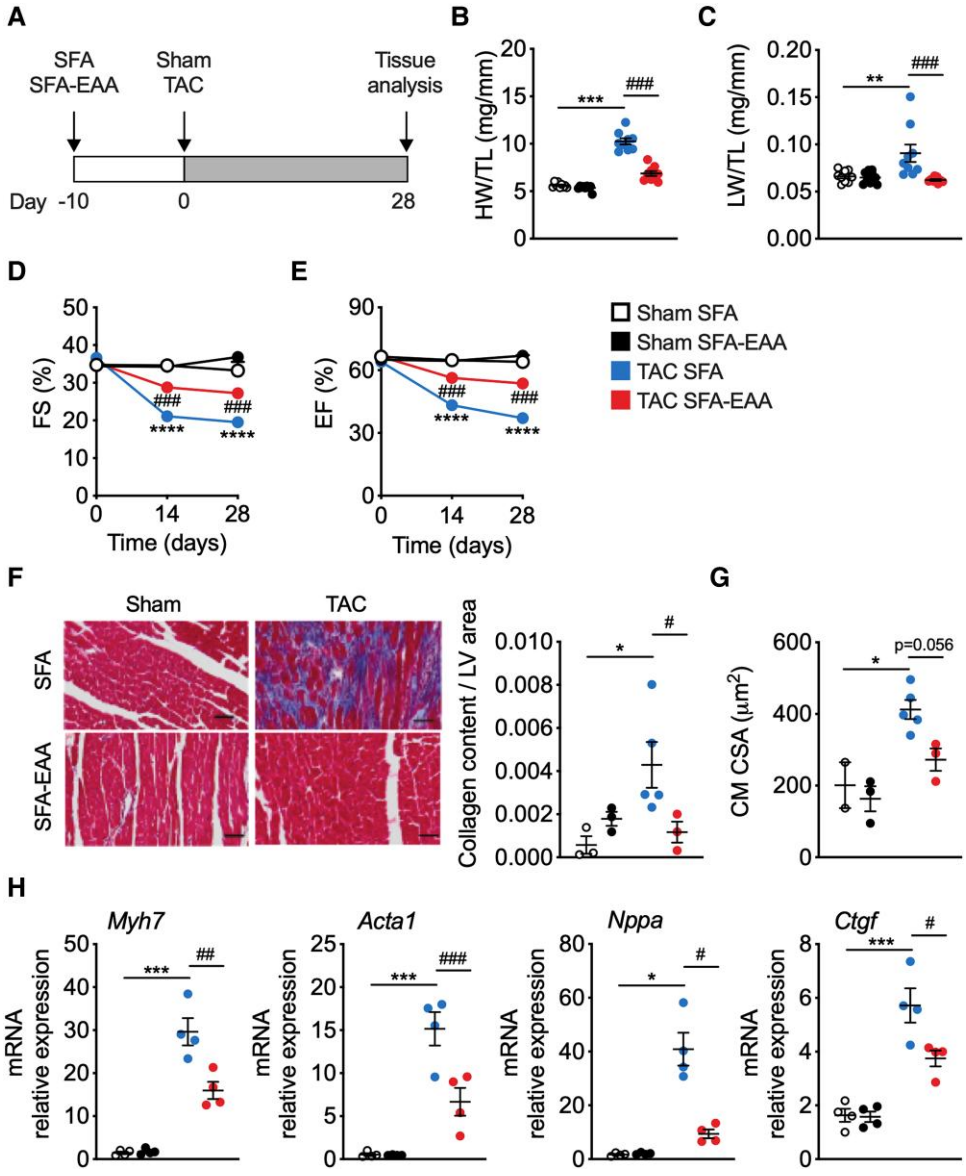

Figure 1 SFA-EAA diet prevents systolic dysfunction caused by pressure overload. (*A*) Schematic overview of SFA and SFA-EAA feeding protocol to male C57BL/6N mice exposed to sham or transverse aortic constriction (TAC) surgery. Mice were fed with the two diets for 10 days before surgery and for additional 4 weeks after surgery, when cardiac parameters were assessed (if not otherwise indicated). (*B* and *C*) Heart weight (B) and lung weight (C) normalized to tibia length (HW/TL) (LW/TL) ($n = 9$ mice per group). (*D*) Percentage fractional shortening (FS %) and (*E*) relative ejection fraction (EF %) in sham- and TAC-operated mice fed with SFA or SFA-EAA diet were quantified by echocardiography ($n = 10$ mice per group). (*F*) Left, representative cross-sections of LV from mice fed with SFA or SFA-EAA diet, subjected to sham or TAC surgery, and stained with Azan's trichrome collagen staining. Scale bars 50 μm. Right, quantification of the fibrotic area showed as the ratio between collagen content vs. area of LV ($n = 3$ mice per group). (*G*) Quantification of cardiomyocyte cross-sectional area (CSA) using wheat germ agglutinin (WGA) staining. (*H*) Gene expression analysis (qRT-PCR) of hypertrophy and fibrosis markers in LV tissue ($n = 4$ animals per group). All data are presented as mean ± SEM. $^{*}P < 0.05$, $^{**}P < 0.01$, and $^{***}P < 0.001$ vs. sham-operated mice fed with SFA diet; $^{\#}P < 0.05$, $^{\#\#}P < 0.01$, and $^{\#\#\#}P < 0.001$ vs. TAC-operated mice fed with SFA diet; comparison was performed by two-way ANOVA followed by post hoc Tukey's test.

2.8 Isolation of mitochondria and oxygen consumption measurement

Mitochondria from LV were isolated as described[19] with some modifications. Briefly, LVs were excised, minced with scissors in 10 mM PBS-EDTA, and spun down. Supernatant was discarded, tissue pellet were resuspended in Trypsin-EDTA (Sigma-Aldrich) and incubated 10 min on ice. Trypsin inhibitor (Sigma-Aldrich) was then added and the mixture was briefly spinned. Supernatant was removed and pellet was homogenized with a glass Potter Elvehjem teflon pestle in 0.3 M sucrose, 10 mM Na-Hepes, 0.2 mM EDTA, 1 mM EGTA, 0.1% bovine serum albumin, pH 7.2, and centifuged at 600 *g* for 10 min at 4°C to spin down nuclear fraction. Supernatant was then collected and centrifuged again at 8 500 *g*

for 10 min at 4°C. Pellet was washed with homogenization buffer, briefly re-centrifuged at 14 000 g for 5 min at 4°C and resuspended in a small volume of homogenization buffer. Mitochondrial oxygen consumption rate (OCR) was measured in a gas-tight vessel equipped with a Clark-type oxygen electrode (Rank Brothers Ltd., Cambridge, UK) at 30°C. Mitochondria were incubated in respiration medium (0.25 M Sucrose, 20 mM Na-Hepes, 0.4 mM EGTA, 3 mM $MgCl_2$, 5 mM KH_2PO_4, 0.1% bovine serum albumin pH 7.2). Glucose- or fatty acid oxidation-dependent OCRs were measured in presence of pyruvate or palmitoyl-carnitine, respectively. The following substrates were used in sequence: 2.5 mM malate, 5 mM pyruvate (or 40 µM palmitoyl-CoA plus 2.5 mM carnitine), 100 µM ADP, and 0.01 mg/mL oligomycin (all from Sigma-Aldrich). ADP-stimulated oxygen consumption was used to calculate state 3 (coupled) respiration, and OCR after oligomycin addition was used to measure uncoupled respiration. Carbonyl cyanide-4-trifluoromethoxy phenylhydrazone (FCCP; Sigma-Aldrich) was subsequently added (500 nM) in the presence of oligomycin to obtain the maximal respiration rate. At the end of the measures, mitochondrial suspension was recovered and OCRs were then normalized to mitochondrial protein amount.

2.9 Metabolomics analysis

Non-targeted metabolite profiling, peak identification, and curation was performed by Metabolon (Durham, NC, USA). Samples were prepared using the automated MicroLab STAR® system from Hamilton Company in the presence of several recovery standards for QC purposes. Biochemicals were extracted and analyzed by ultrahigh performance liquid chromatography-tandem mass spectroscopy (UPLC-MS/MS) in four ways: (i) acidic positive ion conditions (water and methanol), optimized for hydrophilic compounds; (ii) acidic positive ion conditions (water, methanol and acetonitrile), optimized for hydrophobic compounds; (iii) basic negative ion conditions; (iv) negative ionization. Raw data were extracted, peak-identified and QC processed using Metabolon's hardware and software. Metabolites were identified by comparison to a library of purified standards with retention time/index, mass to charge ratio (m/z) and chromatographic data (MS/MS spectral data). Peaks were quantified using area-under-the-curve and normalized by amount of starting material (tissue).

2.10 RNA and DNA purification, gene expression, and mtDNA analysis by qPCR

Total RNA was isolated from LV samples using RNeasy Mini Kit (Qiagen) and treated with DNase according to the manufacturer's protocol. cDNA was synthesized using an iScript cDNA Synthesis Kit (Bio-Rad Laboratories). and amplified by real-time quantitative PCR with iTaq Universal SYBR Green SuperMix (Bio-Rad Laboratories) on a CFX Connect Real-Time PCR System (Bio-Rad Laboratories). For mitochondrial DNA (mtDNA) analysis, total DNA was extracted with the QIAamp DNA extraction kit (QIAGEN). mtDNA was amplified using primers specific for the mitochondrial D-Loop region and normalized to genomic DNA by amplifying the first intron of the *β-actin* nuclear gene. Expression levels of both mtDNA and target genes were analyzed using comparative CT methods, and mRNA expression was normalized to *Gapdh*. qRT-PCR primers are listed in Supplementary material online, *Table S3*.

2.11 RNA-sequencing and data analysis

RNA from two biological replicates was isolated using the RNeasy Mini Kit (Qiagen) and treated with DNase according to the manufacturer protocol. Total RNA quality was evaluated using LabChip GXTouch HT with HT DNA 5 K/RNA/CZE LabChip (Perkin Elmer) according to the manufacturer's instructions. RNA-seq libraries were created using the TruSeq Stranded mRNA Sample Prep Kit (Illumina, San Diego, USA) with 96 dual indexes, starting from 400 ng of RNA. Paired end sequence reads (75 bp in length) were generated on a NextSeq 500 (Illumina, San Diego, USA). The sequencing reads were processed to remove Illumina barcodes and aligned to the Ensembl *Mus musculus* reference genome (build GRCm38.87) using STAR v.2.5.1b with default parameters (https://academic.oup.com/bioinformatics/article/29/1/15/272537?login=false). Differential expression analysis was performed using the GLM approach implemented in the R/Bionconductor[20] edgeR v3.24.3 package (FDR ≤ 0.05).[21] Functional enrichment was performed with the function enrichPathway of clusterProfiler v3.10.1 R package (https://www.ncbi.nlm.nih.gov/pmc/articles/PMC3339379/) against Reactome pathway database ($P \leq 0.01$). Complete RNA-sequencing data set are available from the Gene Expression Omnibus (GEO) under the accession number GSE137669.

2.12 Carnitine acetyltransferase enzymatic activity

Carnitine acetyltransferase (CrAT) assay was performed as described.[22] Briefly, LVs were homogenated in T-PER buffer and diluted 1:10 in assay buffer (50 mM Tris-HCl, 1 M EDTA, 0.45 mM acetyl-CoA, 0.1 mM DTNB; pH = 7.8). After 2 min of baseline measurement, 5 mM L-carnitine was added, and CrAT enzymatic activity was assessed by measuring the rate of reduction of DTNB (412 nm) by the free CoA liberated from acetyl-CoA. Results were then normalized to total protein content.

2.13 Valine oxidation assay

Valine oxidation was assessed as reported.[23] LVs (10–20 mg) were minced in 20 mM HEPES, 200 nM adenosine, 2.0% BSA (FA-free), 5 mM glucose, 1 mM Valine (non-radioisotope). Minced tissue was collected and placed in polypropylene tubes with 160 µCi/mmol [1-^{14}C]valine (50 µCi: MORpure, Avantor, USA) and incubated 1 h at 37°C with shaking. Afterwards, hydrogen peroxide (final concentration 10%) was added and [^{14}C] CO_2 was trapped in filter paper soaked with 300 µL of 1 M benzethonium hydroxide solution for 30 min at room temperature. Radioactivity was then counted by scintillation and data were normalized to mg of tissue.

2.14 *In vitro* model of cardiac hypertrophy and EAAm supplementation

HL-1 cardiomyocytes (Sigma-Aldrich—SCC065) were grown in a complete Claycomb medium supplemented with 10% fetal bovine serum (FBS), 0.1 mM norepinephrine, 100 U/ml penicillin/streptomycin, 2 mM L-glutamine in gelatin/fibronectin-coated flasks (all supplements from Sigma-Aldrich) at 37°C, 5% CO_2. Although HL-1 cells are not ideal for studying cardiomyocytes metabolism, they are, however, widely used to study cardiomyocyte hypertrophy *in vitro*.[24] Endothelin-1 (ET-1) (100 nM in DMSO) (Sigma-Aldrich) was added to cells (80–90% confluent) that were previously deprived for 48 hr of norepinephrine and then serum-starved overnight. For EAA supplementation, HL-1 cells were treated with vehicle or ET-1 as described above or supplemented with an essential amino acid mixture (EAAm) alone or in combination with ET-1 in Claycomb medium without FBS and norepinephrine. The mixture reproduces the stoichiometric ratio of the EAAs in the SFA-EAA defined diet, which, in turn, is based on the blend of AAs that has been previously shown, when supplemented with drinking water, to extend the average life span in mice.[13] After 24 h, cells were harvested for analysis.

2.15 Statistical analysis

For each experiment sample size reflects the number of independent biological replicates and is provided in the figure legend. Sample size was determined on the basis of previous experience. Statistical analyses was performed using unpaired Student's *t*-test for two group analysis or two-way ANOVA followed by post hoc Tukey's test using Prism 6.0 software (GraphPad Software, Inc.). For metabolomics data, a two-way ANOVA (heart) and Welch's two-sample *t*-test (serum) were used to identify biochemicals that differed significantly between experimental groups, and an estimate of the false discovery rate (FDR) is calculated to take into account the multiple comparisons that normally occur in metabolomic-based studies. A value of $P < 0.05$ was considered statistically significant.

3. Results

3.1 SFA-EAA diet prevents HFrEF

To test the effects of the SFA-EAA diet on heart function in response to pathological stress, we fed mice with the SFA or SFA-EAA diet for 10 days and then subjected them to TAC to induce LV pressure overload or sham surgery (*Figure 1A*). Following surgery, mice fed with the SFA-EAA diet for further 4 weeks showed attenuated features of HFrEF progression compared with mice fed with the SFA diet. In particular, cardiac enlargement, significant in TAC mice fed with SFA diet, was absent in TAC mice fed with the SFA-EAA diet: as a consequence, in this latter group, heart and LV weight were similar to those of sham controls when normalized to tibial length. (*Figure 1B*, Supplementary material online, *Figure S1A*), as well as normalized the increased ratio of lung weight/tibial length occurring in TAC animals fed with SFA diet *(Figure 1C)*. An improvement in cardiac performance upon SFA-EAA feeding of TAC-operated mice was evident with transthoracic echocardiography, showing values of fractional shortening (FS), ejection fraction (EF), and left ventricular internal diameter end diastole (LVIDd) and left ventricular internal diameter end systole (LVIDs) comparable with those observed in sham-operated mice fed with SFA diet (*Figure 1D and E,* Supplementary material online, *Figure S1B* and Supplementary material online, *Table S4*). The improved cardiac phenotype of SFA-EAA-fed mice was accompanied by reduced LV interstitial fibrosis and cardiac stress markers compared to those fed with the SFA diet upon pressure overload (*Figure 1F* and *H*).[25] Furthermore, the TAC-induced increase in cardiomyocytes cross-sectional area (CSA) of SFA-fed mice was also reduced by the SFA-EAA diet (*Figure 1G*).

To determine whether the preventive effect of the SFA-EAA diet was indeed due to its specific amino acid composition and not only to free amino acid substitution *per se* or dietary protein deprivation, we generated another engineered diet in which a mixture of free amino acids designed on the amino acid profile of casein replaced the protein component as in the SFA-EAA diet (we referred to this engineered diet as SFA-CAA; Supplementary material online, *Table S1*). Of note, there was no protective action on the cardiac function when mice fed with the SFA-CAA diet were TAC-operated (see Supplementary material online, *Figure S2A–E* and Supplementary material online, *Table S5*). Thus, we decided to compare the SFA-EAA diet to the SFA diet as control. Overall, these results indicate that our specific dietary intervention effectively prevents the development of LV hypertrophy upon pressure overload.

3.2 SFA-EAA diet ameliorates preestablished HFrEF

We next asked whether the SFA-EAA diet could block the progression of cardiac dysfunction in the preestablished HFrEF. Two weeks after surgery, when the cardiac function was significantly reduced in TAC- compared to sham-operated mice, the animals were randomized to receive either the control SFA or the SFA-EAA diet for six weeks (see Supplementary material online, *Figure S3A*). We found that the SFA-EAA diet significantly blocked HF progression; the ratio of heart weight/tibial length, which was increased in TAC-SFA animals, was reduced considerably by SFA-EAA feeding; furthermore, the TAC-SFA-induced augmented ratio of lung weight/tibial length, also tended to be blunted by SFA-EAA, albeit not significantly (see Supplementary material online, *Figure S3B and C*). Notably, SFA-EAA-fed mice did not display any further reduction in FS and EF, resulting in a considerably increased LV function by the end of the experiment compared with SFA-fed mice (see Supplementary material online, *Figure S3D–F* and Supplementary material online, *Table S6*). Moreover, cardiac stress markers' expression was significantly induced in controls and greatly reduced by the SFA-EAA diet (see Supplementary material online, *Figure S3G*). Thus, the SFA-EAA diet consumption substantially benefits HF progression even when the disease is already established. Although we did not measure the survival rate in mice subjected to sham/TAC surgery before or after feeding SFA or SFA-EAA diet, our previous results[13,26] together with recent data which show that both genetic and pharmacological stimulation of mitochondrial biogenesis/activity increased the survival of post-TAC mice,[27] suggest that the substituted diet may extend survival after TAC; however, further experiments will investigate this critical topic.

3.3 Effects on the whole-body metabolism

Both mice fed with the SFA-EAA diet as in *Figure 1A* (*i.e.* preventive protocol) and Supplementary material online, *Figure S3A* (*i.e.* therapeutic protocol) showed a slight decrease in body weight compared to SFA-fed mice (see Supplementary material online, *Figure S4A*). Similarly, feeding the SFA-EAA diet increased whole-body glucose tolerance compared to the SFA diet in sham- and TAC-operated mice (see Supplementary material online, *Figure S4B*). Likewise, when mice were challenged with an insulin tolerance test, the hypoglycaemic effect of insulin was more pronounced in mice fed with the SFA-EAA diet compared with SFA-fed animals of both sham and TAC groups (see Supplementary material online, *Figure S4C*). These results align with those we previously described in not operated mice.[26] To test whether the dietary manipulation affects cardiac insulin signalling, we determined insulin receptor substrate 1 (IRS1) and Akt activation as indicated by pan-tyrosine phosphorylation assay and serine 473 phosphorylation, respectively, eight weeks after sham and TAC in LV. The pan-tyrosine phosphorylation of IRS1 increased after TAC surgery relative to sham mice fed with the SFA diet, as previously described in chow-fed animals[28] (see Supplementary material online, *Figure S4D*). Notably, the SFA-EAA diet completely prevented this induction. We observed similar results with Akt (Ser473) phosphorylation normalized to total Akt (see Supplementary material online, *Figure S4E*). Further analysis showed that neither cardiac TAC surgery nor SFA or SFA-EAA diets affected insulin signalling in both muscle and liver, as indicated by unchanged IRS1 phosphorylation levels in those organs, thus confirming the tissue-specific effect of the SFA-EAA diet on blunting TAC-induced cardiac insulin signalling hyperactivation (see Supplementary material online, *Figure S4F and G*).

Thus, our results suggest that the pressure overload after TAC surgery activates markers of cardiac insulin signalling and that a specific EAA-substituted diet could prevent excessive activation of these markers.

3.4 The metabolic reprogramming induced by the SFA-EAA diet reinstates myocardial energy homeostasis in HFrEF

To clarify the impact of the SFA-EAA diet on systemic metabolism, we performed unbiased metabolomic profiling of plasma from mice subjected to the preventive protocol. Principal component analysis (PCA) showed a clear separation of the two TAC groups according to diet (see Supplementary material online, *Figure S5A*). A total of 23% of detectable metabolites ($n = 159$ of 706)—mostly fatty and amino acids—were differentially regulated in response to the SFA-EAA diet (see Supplementary material online, *Figure S5B*). Among the central metabolic pathways regulated by the dietary regimens, the SFA-EAA diet augmented the BCAA (*i.e.* valine, leucine, and isoleucine) metabolism pathway beyond lysine degradation and phenylalanine, tyrosine, and tryptophan biosynthesis (see Supplementary material online, *Figure S5C*). Accordingly, BCAA and many branched-chain α-keto acid (BCKD) oxidation products were upregulated in the plasma of TAC-operated mice fed with the SFA-EAA diet (see Supplementary material online, *Figure S5D*). In line with our previous data,[26] markers of kidney function, such as creatinine and blood urea nitrogen, were unaltered by SFA-EAA feeding (data not shown).

We thus focused on unbiased metabolomic profiling of cardiac tissue, examining the LV obtained from sham- or TAC-operated mice fed with the two diets as in *Figure 1A* (preventive protocol). First, we examined the effects of dietary regimens on tissue metabolites. PCA showed a clear separation between diets in both sham- and TAC-operated animals (*Figure 2A* and *B*), suggesting that the SFA-EAA diet consumption results in a unique metabolic state of cardiac tissue. A total of 26 and 27% of detectable

metabolites ($n = 146$ and 155 of 572) were significantly upregulated or downregulated in response to the SFA-EAA diet in sham- and TAC-operated mice, respectively (*Figure 2C* and *D*). These included amino acids and fatty acids in the sham group (*Figure 2E*) and amino acids, fatty acids, and carbohydrates in the TAC group (*Figure 2F*). Next, we examined the metabolomic changes elicited by the previous exposure to different dietary interventions in TAC-operated mice on this subset of metabolites. While in SFA-fed mice, the TAC intervention induced changes in the levels of 206 metabolites in total (37% upregulated—mostly carbohydrates and amino acids—and 63% downregulated—mostly fatty acids) (*Figure 3A* and *B*), in SFA-EAA-fed animals, TAC changed the total levels of only 114 metabolites (23% upregulated—mainly fatty acids—and 77% downregulated—mainly fatty acids and amino acids) (*Figure 3A–C*). Notably, the SFA-EAA diet restored the levels of 88 and 69% metabolites, upregulated and downregulated, respectively, in the failing heart (*Figure 3D*). In mice fed with the SFA diet, TAC increased central metabolic pathways, including glycolysis, pentose phosphate pathway, and methionine metabolism (*Figure 3E*), which were all blunted by the SFA-EAA diet. In particular, the levels of the glycolytic intermediates fructose-6-phosphate, fructose-1,6-diphosphate, glucose-1-phosphate, glucose 6-phosphate, fructose 6-phosphate, pyruvate, and lactate, and those of pentose phosphate pathway metabolites sedoheptulose-7-phosphate, ribulose/xylulose-5-phosphate, and 6-phosphogluconate—markedly enriched in TAC-operated mice fed with SFA diet—were reduced to levels similar to those observed in control sham-operated mice fed with SFA diet (*Figure 3F*).

Additionally, the cardiac acylcarnitine levels were significantly lower in TAC-operated mice fed with the SFA diet than in sham-operated mice fed with the SFA diet (see Supplementary material online, *Figure S6*). However, the SFA-EAA diet consumption blunted this effect reversing TAC-induced changes. Similarly, the SFA-EAA diet dampened the TAC-increased levels of polyamines, such as putrescine and spermidine—metabolites indicative of the fibrotic response, known to be associated with pressure overload cardiac dysfunction (*Figure 3G*).[29,30] Together, these results suggest that the amino acid-substituted diet may promote a more energy-efficient oxidative metabolism in the failing heart. BCAA oxidation seems among the most prominently affected pathways (*Figure 3H*).

3.5 Transcriptomic reprogramming induced by the SFA-EAA diet

We next sought to determine how this cardiac metabolic shift affects heart function and explains the beneficial effects observed with the SFA-EAA diet. PCA analysis of cardiac transcriptome showed that the gene expression patterns in LV of sham-operated mice (preventive protocol as in *Figure 1A*) were mainly similar between diets. In contrast, in LV of TAC-operated animals, the patterns displayed extremely distinct profiles (*Figure 4A*). Notably, TAC mice fed with the SFA-EAA diet hierarchically clustered more closely with SFA- and SFA-EAA-fed sham mice than with the SFA-TAC mice (*Figure 4B*). Comparative analysis revealed that the SFA-EAA diet significantly regulated 94 genes in sham- and 305 genes in TAC-operated mice. Consistent with previous results, pressure overload extensively modulates gene expression in LV,[31] remarkably, a total of 36% of these transcripts ($n = 185$ of 516) was entirely restored by the SFA-EAA diet (*Figure 4C*). The volcano plot demonstrated that feeding the SFA-EAA diet strongly dampened multiple TAC-upregulated stress genes (*e.g. Myh7*, *Acta1*, *Nppa*, and *Ctgf*) (*Figure 4D*, left panel). Similarly, numerous TAC-downregulated genes were rescued by the SFA-EAA, including those related to carbohydrate metabolism, tricarboxylic acid (TCA) cycle, and BCAA catabolism (*Figure 4D*, right panel). According to the pathway analysis of genes rescued by the SFA-EAA diet, several processes implicated in HF pathophysiology were identified, including glucose metabolism, extracellular matrix organization, immune system response, and membrane potential regulation (*Figure 4E*). Thus, the SFA-EAA diet in TAC mice appears to induce a transcriptional cardiac response with a pattern opposite to that of pressure overload, which involves the expression of stress and metabolic genes known to play a critical role in the failing heart.

3.6 Mitochondrial respiration and BCAA oxidation

Joint pathway analysis of transcriptomics and metabolomics data with Integrated Molecular Pathway Level Analysis (IMPaLA)[32] revealed respiratory electron transport chain (ETC), TCA cycle, and BCAA oxidation as the most coherent pathways (*Figure 4F*). Of note, the SFA-EAA diet restored both BCAA catabolite levels (*Figure 4G*) and expression of BCAA oxidation genes (*Figure 4H*), which were upregulated and downregulated, respectively, in LV of mice undergone to TAC surgery. In addition, the SFA-EAA diet rescued mRNA levels of the *peroxisome proliferator-activated receptor γ coactivator 1α* (PGC-1α) and *transcription factor A* (Tfam) (mitochondrial biogenesis regulators), *cytochrome c oxidase subunit IV* (COX IV) and *cytochrome c* (Cyt c) (mitochondrial respiratory ETC), and *optic atrophy 1* (OPA1) (inner mitochondrial membrane, which regulates mitochondrial fusion and cristae structure), as well as mitochondrial DNA (mtDNA) amounts, in LV of TAC mice (see Supplementary material online, *Figure S7A and B*), suggesting the restoration of TAC-induced mitochondrial impairment. Although impaired mitochondrial oxidation may induce accumulation of acylcarnitines, we observed a lower level (or no change) of several carnitines and acylcarnitines in the energetically compromised myocardium of TAC-operated mice, in line with previous results (see Supplementary material online, *Figure S6*).[33] On the other hand, CrAT activity—which regulates substrate oxidation in mitochondria and cardiac metabolic flexibility—was decreased in TAC mice fed with the SFA diet and restored to control levels by the SFA-EAA diet (*Figure 5A*). Impaired CrAT activity leads to hyperacetylation of mitochondrial proteins leading to mitochondrial dysfunction,[34] furthermore, mitochondrial protein lysine hyperacetylation is observed in the early stages of HF.[35] We thus measured mitochondrial lysine acetylation in cardiac tissue of TAC-operated mice. Compared with sham mice, TAC increased acetyllysine (AcK) residues in SFA but only partially in SFA-EAA-fed animals (*Figure 5B*), further supporting the beneficial effect of the substituted diet on mitochondrial function.

To test this event directly, we assessed respiration in isolated cardiac mitochondria. Pressure overload considerably reduced basal and maximal oxygen consumption of mitochondria isolated from LV of mice fed with the SFA diet (*Figure 5C*). On the contrary, the SFA-EAA diet completely restored basal and maximal respiration in TAC-operated mice without changing oxygen consumption in the sham-operated animals (*Figure 5C*). Of note, this effect was observed only with pyruvate but not with palmitoyl-carnitine-driven mitochondrial respiration, suggesting a selective restoration of mitochondrial glucose oxidation (see Supplementary material online, *Figure S7C*). Ultrastructure analysis also revealed that the SFA-EAA diet corrected mitochondrial damage in the LV cardiomyocytes of TAC-operated mice. While in the SFA-TAC mice, the cardiac mitochondria were numerous, enlarged, spherical, with the sign of fission—as widely reported in the literature,[36,37] their appearance in the SFA-EAA-TAC mice was comparable to SFA-sham mice, with a more heterogeneous and elongated morphology (*Figure 5D*). Of note, LV transverse sections showed a massive accumulation of amorphous material—damaged sarcomeric myofilaments and other constituents—and Z-lines completely deranged in SFA-TAC mice (see Supplementary material online, *Figure S7D*). These damage signs were absent in TAC-operated mice fed with the SFA-EAA diet (see Supplementary material online, *Figure S7D*).

To investigate further the mechanism underlying the regulation of mitochondrial substrate utilization by the substituted diet, we established an *in vitro* model of cardiomyocyte hypertrophy in which endothelin-1 (ET-1) hypertrophic HL-1 cardiomyocytes were supplemented with an EAA-enriched mixture (EAAm) stoichiometrically equivalent to the amino acid content of the SFA-EAA diet. As shown in Supplementary material online, *Figure S7E*), ET-1 increased the expression of *Nppa* and *Nppb*, which were reduced to control levels by EAAm. Besides confirming the efficacy of the *in vitro* model, these data also suggest a cell-autonomous mechanism of action of the designer diet. Furthermore, in line with the results on

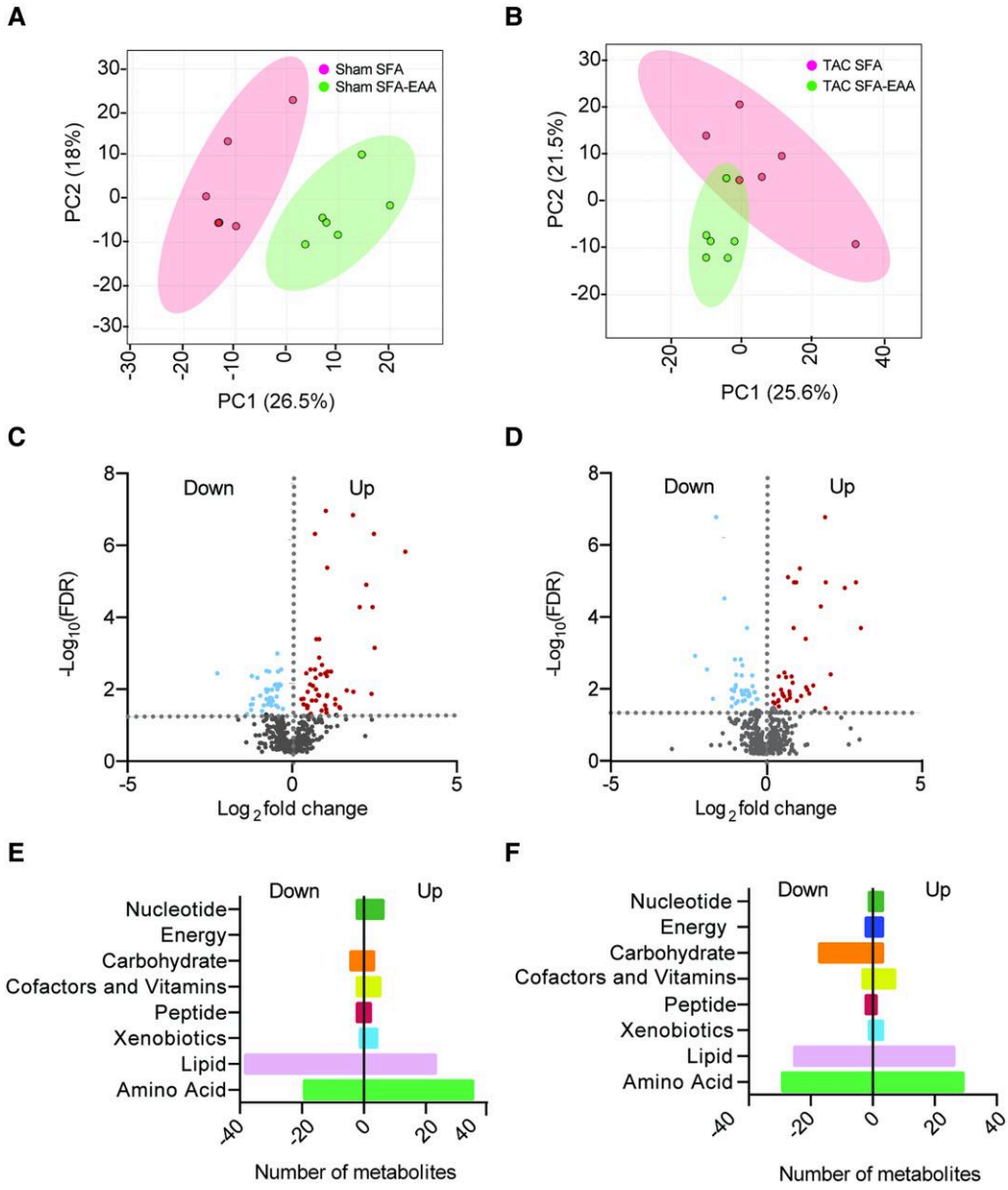

Figure 2 Metabolic reprogramming mediated by the SFA-EAA diet is associated with extensive changes in cardiac metabolite levels related to energy metabolism in sham- and TAC-operated mice. *A* and *B*: Principal component analysis (PCA) of metabolome data. Cardiac tissue (LV) was obtained from sham- (A) and TAC-operated (B) mice fed with SFA or SFA-EAA diet as in *Figure 1A* ($n = 6$ mice per group). (*C* and *D*) Volcano plot showing upregulated (red dots), downregulated (light-blue dots), and unchanged (grey dots) metabolites in LV of sham- (C) and TAC-operated (D) mice fed with SFA-EAA vs. SFA diet ($n = 6$ mice per group; $P < 0.05$). *E* and *F*: Biochemical classification of metabolites in LV of sham- (E) and TAC-operated (F) mice, shown as the number of metabolites for each class significantly modulated by SFA-EAA vs. SFA diet ($n = 6$ mice per group). Statistical analysis was performed with two-way ANOVA and an estimate of the false discovery rate (FDR) for multiple comparisons.

mitochondrial biogenesis markers, while ET-1 downregulated COX IV protein expression, EAAm restored it (see Supplementary material online, *Figure S7F*). Most importantly, EAAm supplementation normalized the ET-1-induced increase in Ser293-phosphorylation of the α1 subunit of pyruvate dehydrogenase complex (PDH) in HL-1 cardiomyocytes, thus confirming, accordingly with the OCR data (*Figure 5C*), the ability of the EAAm to reduce the impairment in pyruvate oxidation and therefore to improve metabolic flexibility in mitochondria of hypertrophic cardiomyocytes (see Supplementary material online, *Figure S7F*). However, the pyruvate dehydrogenase kinase 4 (PDK4) mRNA levels were unchanged by ET-1 and EAAm (data not shown), thus suggesting that in our *in vitro* model, the regulation of PDH activity could proceed through a mechanism independent of PDK4 transcription.

The entire catabolic pathway of BCAAs is located in mitochondria. Unexpectedly, given the high content of BCAAs, but consistent with the increased mitochondrial function, the SFA-EAA diet renormalized increased BCAA levels in LV of TAC-operated mice (*Figure 4G*). It also restored the cardiac levels of many BCAA oxidation products and BCAA oxidative enzymes in the failing heart (*Figure 4G* and *H*). Accordingly, valine oxidation was decreased by pressure overload in SFA-fed mice and

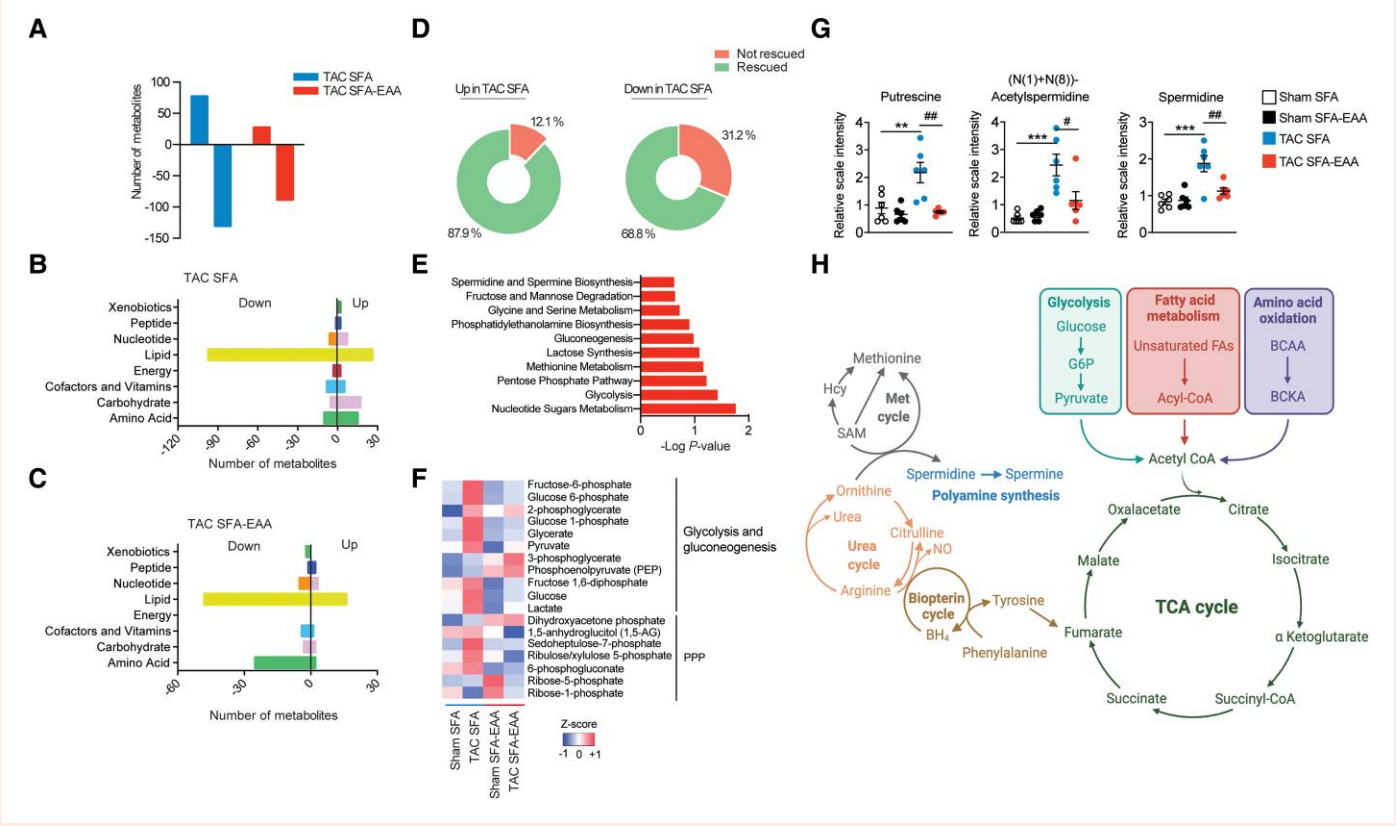

Figure 3 SFA-EAA diet preserves cardiac metabolism upon pressure overload. (*A*) Bars represent the number of metabolites significantly upregulated or downregulated ($P \leq 0.05$) by TAC in LV of mice fed with SFA and SFA-EAA diet as in *Figure 1A* ($n = 6$ mice per group). (*B* and *C*) Biochemical classification of metabolites in LV of TAC-operated mice, shown as the number of metabolites for each class significantly modulated by SFA (B) and SFA-EAA diet (C) ($n = 6$ mice per group). (*D*) Percentage of metabolites in LV of SFA-fed mice, upregulated (left) or downregulated (right) by the pressure overload and that were rescued or not by the SFA-EAA diet ($n = 6$ mice per group). (*E*) Pathway-enrichment analysis of metabolites significantly ($P \leq 0.05$) increased upon TAC in the SFA group ($n = 6$ mice per group). (*F*) Heatmap of cardiac metabolites showing the levels (red = high, blue = low) of differentially regulated intermediates involved in glycolytic, gluconeogenesis, and pentose phosphate pathway in sham- and TAC-operated mice fed with SFA and SFA-EAA diet ($n = 6$ mice per group). (*G*) Polyamine metabolite levels in LV of sham- and TAC-operated mice fed with SFA and SFA-EAA diet. The relative scale intensity was determined by rescaling each metabolite ($n = 6$) to set the median equal to 1.0. All data are presented as mean ± SEM. $^{**}P < 0.01$ and $^{***}P < 0.001$ vs. sham-operated mice fed with SFA diet; $^{\#}P < 0.05$, $^{\#\#}P < 0.01$, and $^{\#\#\#}P < 0.001$ vs. TAC-operated mice fed with SFA diet. Statistical analysis was performed with two-way ANOVA followed by Tukey's post hoc test (panel G) and Fisher's Exact Test (E). (*H*) Schematic diagram showing the main metabolic pathways affected by the SFA-EAA diet in cardiac tissue of TAC-operated mice. Diagram was created with BioRender.com.

recovered by the SFA-EAA diet (*Figure 6*). Beyond normalizing the TAC-induced BCAA and their catabolite accumulation in cardiac tissue (*Figure 4G*), the substituted diet restored glucose oxidation, which is impaired in the failing heart (*Figures 3F, 5C*). Given that high BCAA level inhibits glucose metabolism and, in reverse, glucose promotes cell growth by suppressing BCAA degradation in cardiomyocytes,[38] we hypothesized that the SFA-EAA diet could reduce the TAC-induced activation of the mechanistic target of rapamycin (mTOR) kinase. The BCAA leucine promotes activation of mTOR, which stimulates protein synthesis—leading to development of pathological hypertrophy of adult hearts in vivo.[38] Phosphorylation of eukaryotic translation initiation factor 4E (eIF4E)-binding protein (4E-BP1) and S6 ribosomal protein (S6), two mTOR complex 1 (mTORC1) downstream targets, was lower in TAC-operated mice fed with SFA-EAA than SFA diet (see Supplementary material online, *Figure S8*). Together, these results—in line with previous findings[39–41]—strongly indicate that a reduced BCAA catabolism promotes BCAA accumulation, mTOR activation, and cardiac hypertrophy in TAC mice. Moreover, our results suggest that the SFA-EAA-activated mitochondrial biogenesis and function could reduce the cardiac BCAA levels, mTOR activity, and dysfunction.

3.7 The beneficial effects of the SFA-EAA diet in HFrEF require protein phosphatase PP2Cm

BCAAs are reversibly converted by mitochondrial branched-chain aminotransferase (BCAT2) into branched-chain α-keto acids, which are irreversibly decarboxylated by the branched-chain α-ketoacid dehydrogenase (BCKDH) complex and other enzymes into TCA cycle intermediates.[42] The BCKDH complex is inactive when phosphorylated by branched-chain α-keto acid dehydrogenase kinase (BCKDK) and active when dephosphorylated by 2C-type serine-threonine protein phosphatase (PP2Cm, encoded by *Ppm1k*) (*Figure 7A*).[16,43] We confirmed a reduced expression of these critical BCAA catabolic enzymes (except for BCKD kinase) in the failing heart of SFA-fed mice (*Figure 7B* and *C*).[39] However, we observed a coordinated increase of the same set of proteins in TAC mice fed with the SFA-EAA diet (*Figure 7B* and *C*). In contrast, no significant modification of their expression was evident in white adipose tissue (except for BCAT2), liver (except for BCAT2 and PP2Cm), and skeletal muscle of sham- and TAC-operated mice on the various dietary regimens (see Supplementary material online, *Figure S9A–C*).

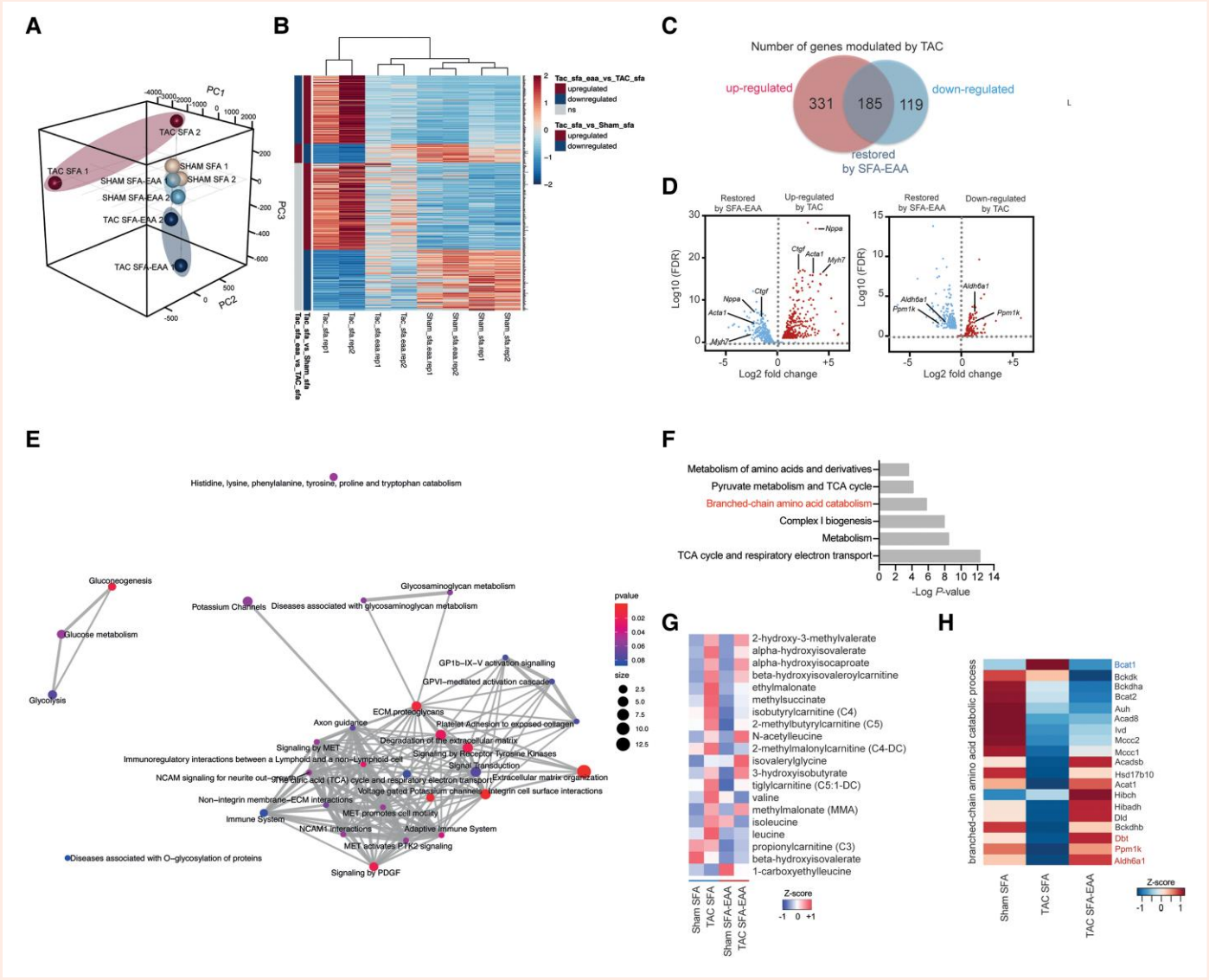

Figure 4 SFA-EAA diet preserves cardiac transcriptomic profile upon pressure overload. (*A*) Three-dimension principal component analysis (3D PCA) of RNA-seq data in LV samples obtained from sham- and TAC-operated mice fed with SFA or SFA-EAA diet as reported in *Figure 1A*. (*B*) Heatmaps of cardiac transcripts showing the levels (red = high, blue = low) of differentially regulated genes following sham and TAC surgery in mice on the different dietary regimens. Statistical criteria is false discovery rate (FDR < 0.05) ($n = 2$ mice per group). The upregulated (dark red), downregulated (dark blue), or not changed (grey) gene groups are also reported in TAC-operated mice fed with SFA-EAA vs. SFA diet or in TAC- vs. sham-operated mice fed with SFA diet (the two left columns). (*C*) Venn diagram showing upregulated (red circle) and downregulated (blue circle) genes in LV following pressure overload, and the genes entirely restored by the SFA-EAA diet (overlap). (*D*) Volcano plot showing cardiac genes upregulated (red in the left panel) and downregulated (red in the right panel) by TAC surgery and their restoration by the SFA-EAA diet (blue in the left and right panels, respectively) ($n = 2$ mice per group; FDR < 0.05). (*E*) Pathway analysis of cardiac genes significantly modulated by the SFA-EAA diet in TAC-operated mice. The *P*-values indicate the enrichment level of the pathway term; the colour intensity and size indicate the significativity level and the number of proteins included in a single pathway, respectively. (*F*) Joint pathway analysis of transcriptomics and metabolomics data ($n = 6$ mice per group). (*G*) Heatmap of the levels of BCAA catabolites in sham- and TAC-operated mice fed with SFA or SFA-EAA diet ($n = 6$ mice per group). (*H*) Heatmap of the expression profile of BCAA oxidation genes in mice fed with SFA or SFA-EAA diet and subjected to sham or TAC surgery. Differential expression analysis was performed using the GLM approach in edgeR using a false discovery rate (FDR), while pathway analysis was made with Integrated Molecular Pathway Level Analysis (IMPaLA) using a *P*-value from Fisher's Exact Test.

In cardiac tissue, these genes are regulated by the circadian gene Krüppel-like factor 15 (KLF15), which governs the transcriptional regulation of cell proliferation, differentiation, and metabolism; the expression of KLF15 is downregulated in failing hearts.[44] We confirmed that KLF15 was strongly downregulated following TAC in LV—but not in adipose, liver, and muscle (see Supplementary material online Supplementary material online, *Figure S9*)—of mice fed with the SFA diet; in contrast, its cardiac expression was significantly increased by the SFA-EAA diet (*Figure 7B*). Thus, to assess the involvement of BCAA catabolic pathway in the cardioprotective effects of the SFA-EAA diet, we used a mouse model carrying the genetic inactivation of *Ppm1k* (PP2Cm-KO), which lacks the activating phosphatase activity of PP2Cm on the key catabolic BCAA enzyme BCKDHA dehydrogenase. As a result, in PP2Cm-null mice, the subunit E1 of BCKDHA is hyperphosphorylated and inactive in response to

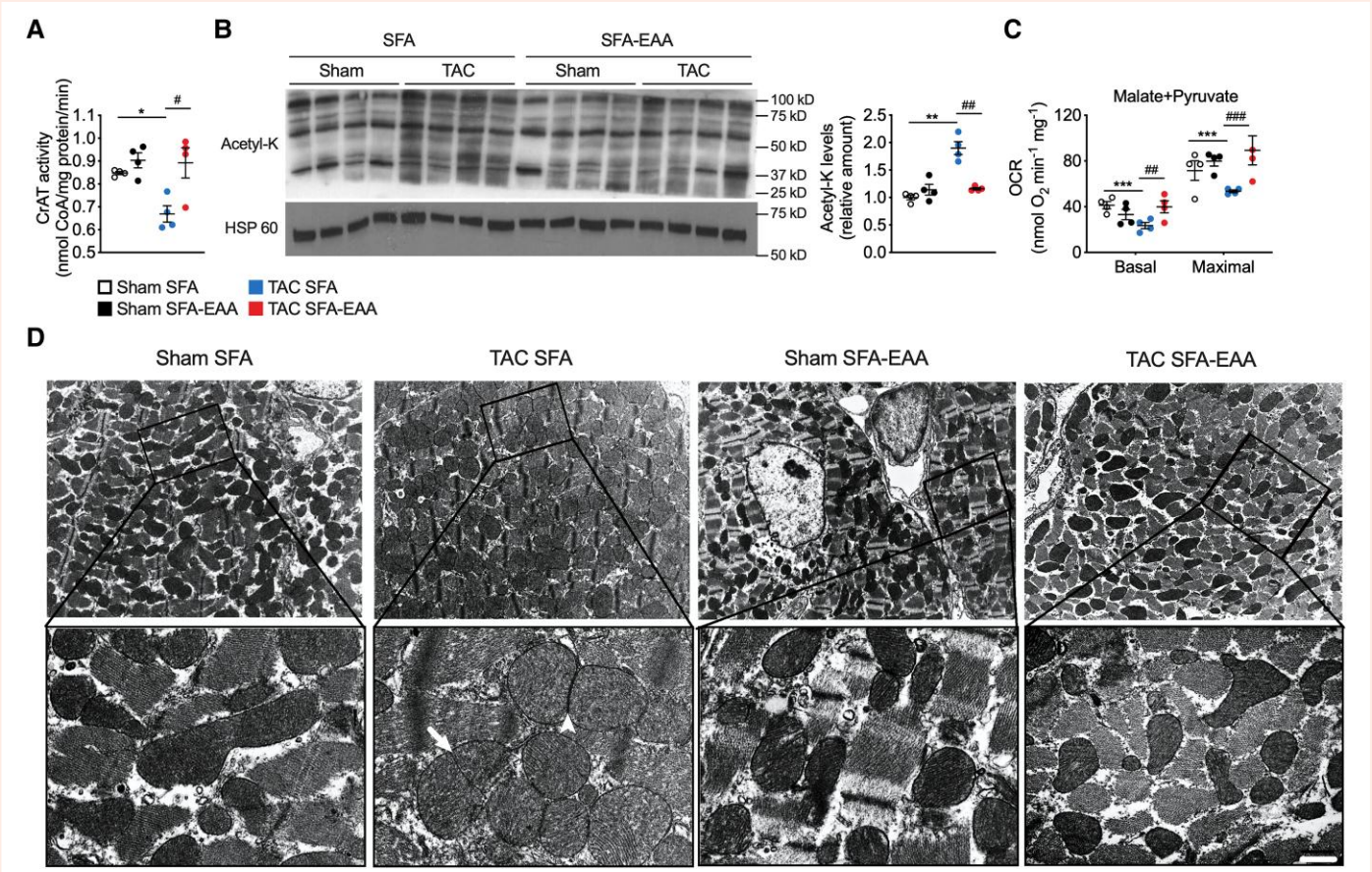

Figure 5 SFA-EAA diet restores TAC-induced mitochondrial dysfunction and structural damage. (*A*) Carnitine acetyltransferase (CrAT) activity in LV obtained from sham- and TAC-operated mice fed with SFA or SFA-EAA diet as reported in *Figure 1A*. CrAT activity is expressed as nmol of free coenzyme A (CoA) released per minute and normalized to mg of total proteins ($n = 4$ mice per group). (*B*) Immunoblot analysis and quantification of lysine acetylation (acetyl-K) of total mitochondrial proteins in LV. One experiment representative of three reproducible ones is shown. (*C*) Oxygen consumption rates (OCRs) in the presence of malate/pyruvate in mitochondria obtained from LV ($n = 4$ mice per group). Basal: ADP-stimulated respiration (state 3); Maximal: maximal respiration (*i.e.* the FCCP-induced uncoupled state) ($n = 5$ mice per group). (*D*) Transmission electron microscopy images showing the mitochondrial morphology in LV. A magnified view of the regions outlined by the lined boxes is reported below. Globular, swollen mitochondria are predominant in TAC-operated mice fed with the SFA diet, with signs of constriction suggesting early stage (arrow) and late-stage (arrowhead) fission events. Scale bar (shown only in TAC SFA-EAA lower pannel), 1.8 μm (upper pannels) and 0.3 μm (lower pannels) ($n = 2$ mice per group). All data are presented as mean ± SEM. $^{*}P < 0.05$, $^{**}P < 0.01$, and $^{***}P < 0.001$ vs. sham-operated mice fed with SFA diet; $^{\#}P < 0.05$, $^{\#\#}P < 0.01$, and $^{\#\#\#}P < 0.001$ vs. TAC-operated mice fed with SFA diet. Statistical analysis was performed using two-way ANOVA followed by the Tukey's post hoc test.

BCKA stimulation, inhibiting the BCAA catabolism.[16] We reasoned that if BCAA catabolic pathway is required for the cardioprotective effect of the SFA-EAA diet in TAC mice, then the SFA-EAA-fed PP2Cm-null animals, in which the BCAA catabolism is impaired, should not show any improvement in cardiac function after TAC. The decrease in heart functional outcomes in these null mice—more evident following TAC than in wild-type mice[39]—was resistant to the beneficial effects of the SFA-EAA diet under the therapeutic protocol (*Figure 7D–G* and Supplementary material online, *Table S7*). Notably, the cardioprotective benefits were absent even if the SFA-EAA diet reduced body weight (*Figure 7H*) and ameliorated whole-body insulin sensitivity in TAC-operated mice compared with the SFA diet.[26,45]

4. Discussion

Current therapies for cardiac hypertrophy and HF are primarily based on pharmacological and surgical approaches mainly for relieving ventricular haemodynamic stress, controlling symptoms, and increasing exercise capacity.[46] However, alteration of metabolic substrate utilization in myocardial tissue is a major hallmark in hypertrophy and HF; reduced metabolic flexibility—that is, the inability to adapt to altered metabolic fuel supplies during diverse physiological and pathophysiological conditions—underlies the majority of morphological and biochemical adaptations which take place in these pathological conditions.[7,47] Therefore, reinstating the compromised metabolic homeostasis and imbalance of substrate utilization is a valuable therapeutic target in failing heart. In this context, dietary manipulation is widely accepted as a beneficial approach to HF; however, most studies obtained unsatisfactory results to progress towards better evidence-based nutritional advice for patients.[48] For instance, adherence to the Mediterranean diet or dietary approaches to stop hypertension (DASH), typically low in saturated fat and high in complex carbohydrates, fish, and vegetables, was associated with improved systolic and diastolic function in individuals with HFrEF and HFpEF. However, their benefits are to be confirmed in large randomized trials.[26,49,50] Alternatively, high-fat, low-carbohydrate ketogenic diets have been found to improve cardiac function

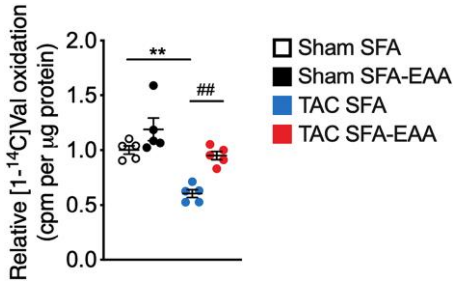

Figure 6 Valine oxidation rate in LV obtained from sham- and TAC-operated mice fed with SFA or SFA-EAA diet as reported in *Figure 1A*, normalized to tissue mass ($n = 3$ mice per group). $^{**}P < 0.01$ vs. sham-operated mice fed with SFA diet; $^{\#\#}P < 0.01$, vs. TAC-operated mice fed with SFA diet using two-way ANOVA followed by the Tukey's post hoc test.

in the failing mouse heart, although not in all studies.[51,52] Additionally, Evangelista et al.[53] observed that a 3-month high-protein diet resulted in more significant reductions of cardiometabolic risks, including systolic and diastolic blood pressure levels, relative to a standard-protein diet in overweight and obese patients with HF and diabetes mellitus; however, further trials of longer duration are needed. Almost all of these interventions are based on a quantitative manipulation of dietary nutrients. Our approach was different: instead of changing dietary macronutrient percentage, we substituted a mixture of free EAAs for protein content. In mice subjected to LV pressure overload as an HFrEF model, consuming a customized diet in which a precise formula of EAAs substitutes for protein content—without changing calorie content and macronutrient percentage—effectively prevents and improves cardiac injury.

Given the high content of BCAAs, the SFA-EAA diet's beneficial cardiac effects may appear unexpected. Indeed, independent associations have emerged that support a direct role for BCAAs in failing heart, particularly in HFrEF.[54] In humans and animals with HF, the BCAA metabolic pathway is downregulated in cardiac tissue, leading to an accumulation of BCAAs and BCKAs,[39] which contributes to HF pathogenesis through a variety of potential mechanisms, including mTOR activation, mitochondrial dysfunction, glucose oxidation defect, and metabolic inflexibility.[54] Nonetheless, many of these links between BCAAs and HF are only correlative and not confirmed by other studies. For example, high plasma BCAA levels at baseline were associated with improvement in LV systolic function in subjects with HFrEF undergoing cardiac resynchronization therapy.[55] Similarly, increased baseline plasma BCAA levels were associated with a decreased risk of developing LV diastolic dysfunction—a marker of future adverse cardiovascular events—in individuals without structural heart disease who were followed up over time with serial echocardiography.[56] These findings suggest that, in specific disease conditions, increased plasma BCAA concentrations might be beneficial.

The association between high BCAA levels and insulin resistance is also long-known.[57] However, there is uncertainty if BCAAs are the cause or effect of IR,[11] and data showing a decrease in glucose tolerance following BCAA supplementation or dietary intake to lean/healthy humans are lacking or conflicting.[58,59] Furthermore, the relationship between BCAAs and IR has been mostly found in obese people and animals,[57,60,61] thus indicating a harmful effect only in the presence of a compromised mitochondrial function. For example, the well-known BCAA supplementation in trained athletes does not induce HF or IR.[58] Our diet, besides BCAAs, also increases the intake of other EAAs. It is therefore coinceivable that activation of mitochondrial activity by the substituted diet could play a relevant role in improving glucose tolerance/insulin sensitivity.[13,26,62]

Mechanistically, the cardioprotective impact of the SFA-EAA diet appears to be mediated through mutually nonexclusive effects on systemic metabolism and local cardiomyocyte signalling. Lower body weight and an improved hypoglycaemic response to insulin might explain the protective and therapeutic effects of the SFA-EAA diet when fed to TAC mice. However, this diet prevents body weight gain also in PP2Cm deficient mice without ameliorating their cardiac performance when exposed to pressure overload. Interestingly, PP2Cm deficient mice have lower body weight and higher insulin sensitivity than wild-type mice but show a more severe deterioration of heart function than controls when exposed to TAC surgery.[45] Overall, these results, together with the *in vitro* results, seem thus to limit the relevance of actions on systemic metabolism in explaining the advantages of the SFA-EAA diet in the failing heart. Notably, the plasma and cardiac levels of BCKA catabolites were upregulated in TAC-operated mice fed with the SFA-EAA diet (see Supplementary material online, *Figure S5D*), and this matched with reduction of the LV levels of BCKAs, which are toxic metabolites in cardiac tissue.[39]

On the other hand, insulin receptor (IR) signalling is activated in hypertrophic cardiac tissue of TAC mice fed with the SFA diet, and IRS1 seems to be involved, as indicated by increased phosphorylation of IRS1 and Akt signalling proteins. These findings confirm those previously reported by Riehle *et al.* in LV of TAC-operated mice.[28] However, our observation that the SFA-EAA diet fully antagonized the activated IR signalling in TAC mice seems relevant, particularly in the suggested synergism between the increased IR activation and the stretch-mediated activation of IRS1/Akt/mTOR signalling pathways leading to hypertrophy in failing heart. An earlier study demonstrated that reducing insulin signalling by lowering circulating insulin or IR or Akt expression attenuated the onset of HF.[63]

The SFA-EAA-induced metabolic and transcription reprogramming reinstates myocardial energy supplies in HFrEF. While plasma and cardiac metabolite clusters following TAC surgery in SFA-fed mice suggest the involvement of multiple biochemical networks widely known in the pathophysiology of failing heart—including impaired glucose, fatty acid, and amino acid oxidation, with increased glycolysis and pentose phosphate pathway[64]—in mice fed with the SFA-EAA diet these clusters are more similar to those observed in the SFA-fed animals after sham surgery. We speculate that the HFrEF-related alteration of the glucose, fat, and amino acid metabolism might be a consequence of the decline of mitochondrial oxidative function or an increased mitochondrial function demand, rather than the reduced activity of single biochemical circuitry and that the global metabolic reprogramming induced by our substituted diet might be linked to a direct action on mitochondria. We have shown previously that the SFA-EAA diet is a potent inducer of mitochondrial biogenesis and function under diverse experimental conditions.[26] Our present results also support this possibility, showing that the TAC-induced decline of expression of PGC-1α and OPA-1, among other genes promoting mitochondrial biogenesis and function,[65,66] is rescued by the SFA-EAA diet. Also, we observed a significant reduction of lysine acetylation of mitochondrial proteins—due to restoration of CrAT activity—and a consequent improvement of mitochondrial function in SFA-EAA-fed TAC mice compared with SFA-fed TAC animals. Notably, CrAT null mice show impaired mitochondrial pyruvate oxidation, glucose sensitivity, and metabolic flexibility, with hyperacetylation and dysfunction of mitochondrial proteins.[22,34] The SFA-EAA diet restored the defective pyruvate/malate-dependent mitochondrial respiration in TAC-operated mice, suggesting the restoration of the mitochondrial glucose oxidation capacity. Thus, one can hypothesize that the ability of the SFA-EAA diet to stimulate CrAT activity might explain the improved glucose oxidation and balance in metabolic substrate utilization of the failing heart. However, because the substrate fluxes do not strongly correlate with both mRNA levels of metabolic enzymes and mitochondrial respiration, our hypothesis will need to be adequately tested in future studies using *in vivo* substrate and glucose flux measurements. Nevertheless, one should note that our metabolomic and transcriptomic results agree with previous investigations describing the

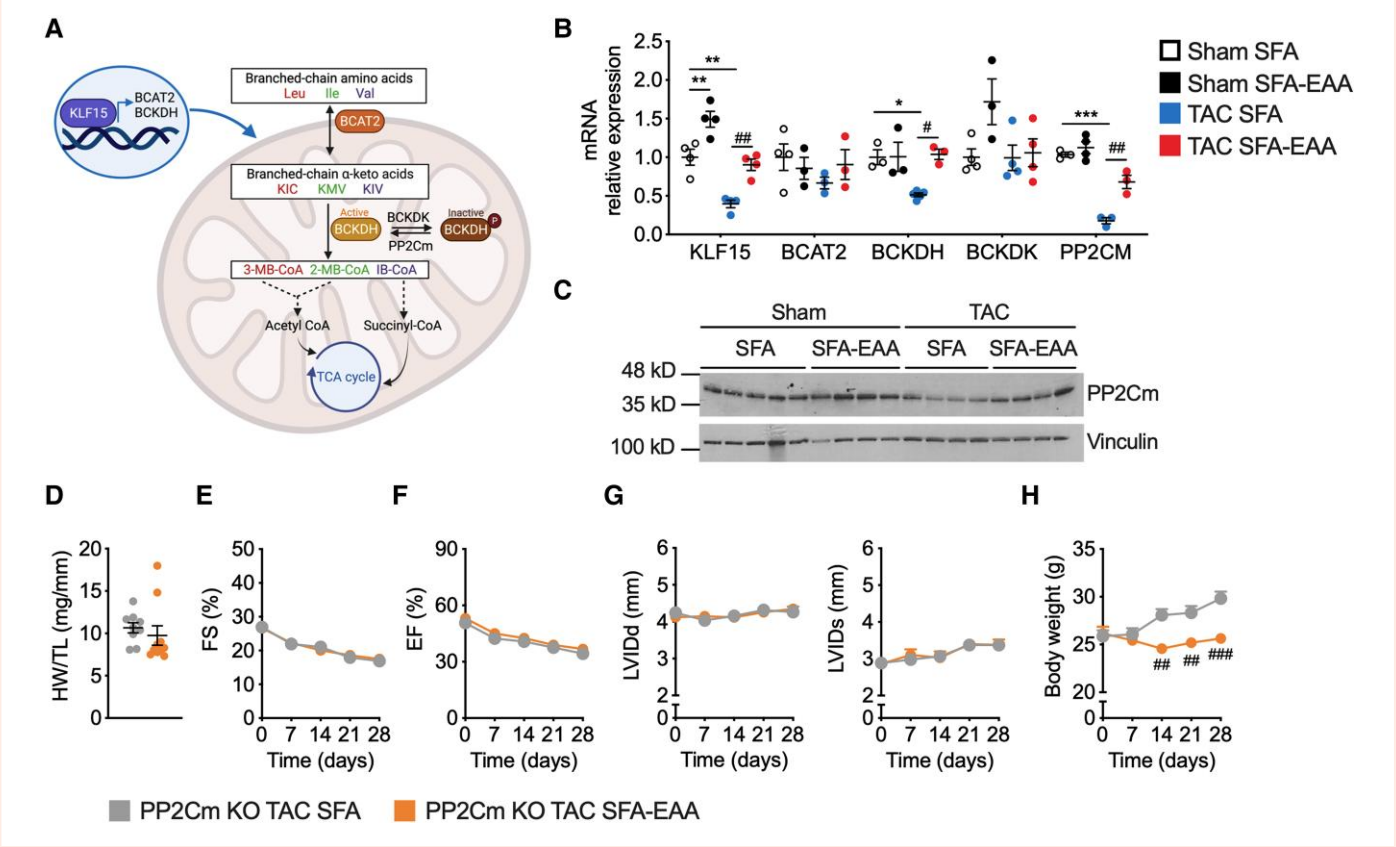

Figure 7 Cardiac BCAA catabolism is required for the beneficial effects of the SFA-EAA diet in HFrEF. (*A*) KLF15 promotes the expression of enzymes crucial to the BCAA oxidation *(e.g.* BCAT2, BCKDH, and PP2Cm), producing acetyl-CoA and succinyl-CoA intermediates of the TCA cycle. KLF15 and BCAA degradation enzymes are downregulated in failing hearts, increasing cardiotoxic branched-chain ketoacids, mTOR activity, and cell growth. Ile, isoleucine; Leu, leucine; Val, valine; BCAT2, mitochondrial BCAA aminotransferase; BCKDH, branched-chain α-ketoacid dehydrogenase complex; BCKDK, branched-chain ketoacid dehydrogenase kinase; PP2Cm, protein phosphatase 2Cm; KIC, ketoisocaproic acid; KMV, α-keto-β-methylvaleric acid; KIV, α-ketoisovaleric acid; 3-MB-CoA, 3-methylcrotonyl-CoA; 2-MB-CoA, 2-methyl-3-hydroxy-butyryl-CoA; IB-CoA, 3-hydroxy-isobutyryl-CoA; TCA, tricarboxylic acid cycle. The BCKDH complex is inactive when phosphorylated by BCKDK and active when dephosphorylated by PP2Cm. (*B*) Relative mRNA levels of BCAA catabolic enzyme genes in LV obtained from sham- and TAC-operated mice fed with SFA or SFA-EAA diet as reported in *Figure 1A* ($n = 3$ mice per group). (*C*) Western blot analysis of PP2Cm in LV of mice fed with SFA or SFA-EAA diet and subjected to sham or TAC surgery. One immunoblot experiment representative of three reproducible ones ($n = 4$–5 mice per group). (*D*) Heart weight normalized to tibia length (HW/TL) in TAC-operated PP2Cm-null mice fed with SFA and SFA-EAA diet as in *Figure 1A* ($n = 10$ mice per group). (*E*) Percentage fractional shortening (FS %) and (*F*) relative ejection fraction (EF %) in TAC-operated PP2Cm-null mice fed with SFA or SFA-EAA diet were quantified by echocardiography ($n = 10$ mice per group). *G*: Left ventricular internal diameter end diastole (LVIDd) (left panel), left ventricular internal diameter end systole (LVIDs) (right panel) and body weight measured once a week (H) in TAC-operated PP2Cm-null mice fed with SFA and SFA-EAA diet ($n = 10$ mice per group). All data are presented as mean ± SEM. $^{*}P < 0.05$, $^{**}P < 0.01$, and $^{***}P < 0.001$ vs. sham-operated mice fed with SFA diet; $^{\#}P < 0.05$, $^{\#\#}P < 0.01$, and $^{\#\#\#}P < 0.001$ vs. TAC-operated mice fed with SFA diet. Statistical analysis was performed with two-way ANOVA followed by Tukey's post hoc test (panel B) and unpaired Student's *t*-test (panel D–H). The cartoon illustration in panel A was created with BioRender.com.

metabolic flux analysis in mice subjected to pressure overload.[67] Moreover, our dietary manipulation could affect systemic or coronary vascular resistance, which may alter metabolic flux,[68] and this will have to be assessed adequately.

Showing the SFA-EAA diet improves glucose oxidation is relevant because high glucose is known to cause the hypertrophic growth of the heart under stress conditions, which ultimately leads to HF. Shao *et al.*[38] suggests that increased intracellular glucose transcriptionally suppresses KLF15 and its downstream genes, resulting in a decreased BCAA degradation. Such a process leads to the accumulation of intracellular BCAA that coincides with mTOR activation. Several observations have been made that KLF15 and BCAA degradation enzymes' expression is downregulated in failing hearts.[39,44] Our findings suggest that the beneficial anti-hypertrophic effects of the SFA-EAA diet in the overload pressure model of HFrEF may be explained partly by modulation of the KLF15-BCAA-mTOR pathway. In particular: (i) the TAC-induced reduction of cardiac KLF15 expression in sham-operated mice is restored to control values in the SFA-EAA-fed animals; (ii) similar results are observed for the expression of multiple genes of amino acid metabolism, including PP2Cm, with (iii) an apparent normalization of BCAA oxidation in cardiac tissue of the TAC-operated mice fed with the SFA-EAA diet; and finally (iv) the TAC-induced mTOR activation is fully inhibited by the SFA-EAA consumption, mimicking the beneficial effects of mTOR inhibitor rapamycin on cardiac hypertrophy.[69,70] Consistently, the substituted diet reduces IR-mTOR-dependent hypertrophic signalling.

Some reports showed therapeutic efficacy of targeting BCAA catabolic flux in TAC-induced HF with BT2 (3,6-dichlorobenzo[b]thiophene-2-

carboxylic acid), a small-molecule inhibitor of BCKDK used to enhance BCAA catabolism. The BT2-treated mice showed significantly preserved cardiac function and structure after TAC, with improved systolic contractility and diastolic mechanics.[71] These therapeutic benefits appeared independent of impacts on LV hypertrophy, suggesting that our SFA-EAA diet may affect additional mechanisms and engage other EAA catabolic pathways, especially those involved in mitochondrial function. Specifically, while BT2 does not increase mtDNA amount in LV in both sham- and TAC-operated mice,[71] the SFA-EAA diet promotes cardiac mitochondrial function.

A few small clinical trials have evaluated the cardiac effects of EAA dietary supplements in patients with HFrEF, with encouraging results on ventricle function and exercise tolerance.[72,73] It remains to investigate whether a marked reduction of protein content and substitution with a specific EAA mixture described in the present paper is therapeutically effective in humans with HFrEF.

5. Conclusion

In summary, the present study indicates that a specific manipulation of dietary amino acids prevents and reverses HFrEF in mice through multiple modes. If extended to humans, such dietary manipulation could positively impact cardiac and systemic metabolic health, favouring the prevention and treatment of HF regardless of calorie consumption.

Author contributions

M.R., G.C., and E.N. designed the research and analyzed the data. P.C. and S.V.R. performed animal surgeries. P.C. and C.G. performed echocardiograms. C.M.G., M.R, C.R., A.F., V.L., M.R., and L.T. performed experiments. I.S., A.G., and S.C. performed and analysed electron microscopy experiments. E.D.P. Provided key reagents and experimental support. P.K. performed bioinformatic analyses. M.R. and E.N. wrote the manuscript with critical revisions from Y.W., H.S. and A.V.

Supplementary material

Supplementary material is available at *Cardiovascular Research* online.

Acknowledgements

The authors thank R. Aquilani (Department of Biology and Biotechnology 'Lazzaro Spallanzani', University of Pavia, Pavia, Italy) for discussion.

Conflict of interest: None declared.

Funding

This work was supported by the European Research Council Advanced Grant (CardioEpigen, # 294609), Cariplo Foundation (grant # 2015-0573), the European Research Area Network on Cardiovascular Diseases (ERA-CVD) (the EXPERT project), the Italian Ministry of Education, University and Research (grant # 2015583WMX) to GC; Professional Dietetics (Milan, Italy) and Fondazione Cariplo (grant no. 2016-1006) to E.N. C.R. was supported by Fondazione Umberto Veronesi.

Data availability

RNA-seq data is available in GEO under the accession number GSE137669. The data underlying this article are available in the article and in its online supplementary material.

References

1. Benjamin EJ, Muntner P, Alonso A, Bittencourt MS, Callaway CW, Carson AP, Chamberlain AM, Chang AR, Cheng S, Das SR, Delling FN, Djousse L, Elkind MSV, Ferguson JF, Fornage M, Jordan LC, Khan SS, Kissela BM, Knutson KL, Kwan TW, Lackland DT, Lewis TT, Lichtman JH, Longenecker CT, Loop MS, Lutsey PL, Martin SS, Matsushita K, Moran AE, Mussolino ME, O'Flaherty M, Pandey A, Perak AM, Rosamond WD, Roth GA, Sampson UKA, Satou GM, Schroeder EB, Shah SH, Spartano NL, Stokes A, Tirschwell DL, Tsao CW, Turakhia MP, VanWagner LB, Wilkins JT, Wong SS, Virani SS. Heart disease and stroke statistics-2019 update: a report from the American heart association. *Circulation* 2019;**139**:e56–e528.
2. Savarese G, Lund LH. Global public health burden of heart failure. *Card Fail Rev* 2017;**3**:7–11.
3. Rossignol P, Hernandez AF, Solomon SD, Zannad F. Heart failure drug treatment. *Lancet*. 2019;**393**:1034–1044.
4. Gheorghiade M, Larson CJ, Shah SJ, Greene SJ, Cleland JGF, Colucci WS, Dunnmon P, Epstein SE, Kim RJ, Parsey RV, Stockbridge N, Carr J, Dinh W, Krahn T, Kramer F, Wahlander K, Deckelbaum LI, Crandall D, Okada S, Senni M, Sikora S, Sabbah HN, Butler J. Developing new treatments for heart failure: Focus on the Heart. *Circ Hear Fail* 2016;**9**: e002727.
5. Zhou B, Tian R. Mitochondrial dysfunction in pathophysiology of heart failure. *J Clin Invest*. 2018;**128**:3716–3726.
6. Neubauer S. The failing heart—an engine out of fuel. *N Engl J Med* 2007;**356**:1140–1151.
7. Stanley WC, Recchia FA, Lopaschuk GD. Myocardial substrate metabolism in the normal and failing heart. *Physiol Rev*. 2005;**85**:1093–1129.
8. Doenst T, Nguyen TD, Abel ED. Cardiac metabolism in heart failure: implications beyond atp production. *Circ Res* 2013;**113**:709–724.
9. Wende AR, Brahma MK, McGinnis GR, Young ME. Metabolic origins of heart failure. *JACC Basic Transl Sci*. 2017;**2**:297–310.
10. Karwi QG, Uddin GM, Ho KL, Lopaschuk GD. Loss of metabolic flexibility in the failing heart. *Front Cardiovasc Med* 2018;**5**:68.
11. Lynch CJ, Adams SH. Branched-chain amino acids in metabolic signalling and insulin resistance. *Nat Rev Endocrinol* 2014;**10**:723–736.
12. Bifari F, Nisoli E. Branched-chain amino acids differently modulate catabolic and anabolic states in mammals: a pharmacological point of view. *Br J Pharmacol*. 2017;**174**:1366–1377.
13. D'Antona G, Ragni M, Cardile A, Tedesco L, Dossena M, Bruttini F, Caliaro F, Corsetti G, Bottinelli R, Carruba MO, Valerio A, Nisoli E. Branched-chain amino acid supplementation promotes survival and supports cardiac and skeletal muscle mitochondrial biogenesis in middle-aged mice. *Cell Metab* 2010;**12**:362–372.
14. Levitan EB, Lewis CE, Tinker LF, Eaton CB, Ahmed A, Manson JE, Snetselaar LG, Martin LW, Trevisan M, Howard B V, Shikany JM. Mediterranean And DASH diet scores and mortality in women with heart failure the women s health initiative. *Circ Hear Fail* 2013;**6**:1116–1123.
15. Hummel SL, Seymour EM, Brook RD, Sheth SS, Ghosh E, Zhu S, Weder AB, Kovacs SJ, Kolias TJ. Low-Sodium DASH diet improves diastolic function and ventricular arterial coupling in hypertensive heart failure with preserved ejection fraction. *Circ Hear Fail* 2013;**6**:1165–1171.
16. Lu G, Sun H, She P, Youn JY, Warburton S, Ping P, Vondriska TM, Cai H, Lynch CJ, Wang Y. Protein phosphatase 2Cm is a critical regulator of branched-chain amino acid catabolism in mice and cultured cells. *J Clin Invest* 2009;**119**:1678–1687.
17. Fontaine DA, Davis DB. Attention to background strain is essential for metabolic research: C57BL/6 and the international knockout mouse consortium. *Diabetes* 2016;**65**: 25–33.
18. Rockman HA, Ross RS, Harris AN, Knowlton KU, Steinhelper ME, Field LJ, Ross J, Chien KR. Segregation of atrial-specific and inducible expression of an atrial natriuretic factor transgene in an in vivo murine model of cardiac hypertrophy. *Proc Natl Acad Sci U S A* 1991;**88**: 8277–8281.
19. Boehm EA, Jones BE, Radda GK, Veech RL, Clarke K. Increased uncoupling proteins and decreased efficiency in palmitate-perfused hyperthyroid rat heart. *Am J Physiol Heart Circ Physiol* 2001;**280**:H977–H983.
20. Gentleman RC, Carey VJ, Bates DM, Bolstad B, Dettling M, Dudoit S, Ellis B, Gautier L, Ge Y, Gentry J, Hornik K, Hothorn T, Huber W, Iacus S, Irizarry R, Leisch F, Li C, Maechler M, Rossini AJ, Sawitzki G, Smith C, Smyth G, Tierney L, Yang JYH, Zhang J. Bioconductor: open software development for computational biology and bioinformatics. *Genome Biol* 2004;**5**:R80.
21. Robinson MD, McCarthy DJ, Smyth GK. Edger: a bioconductor package for differential expression analysis of digital gene expression data. *Bioinformatics* 2009;**26**:139–140.
22. Muoio DM, Noland RC, Kovalik JP, Seiler SE, Davies MN, Debalsi KL, Ilkayeva OR, Stevens RD, Kheterpal I, Zhang J, Covington JD, Bajpeyi S, Ravussin E, Kraus W, Koves TR, Mynatt RL. Muscle-specific deletion of carnitine acetyltransferase compromises glucose tolerance and metabolic flexibility. *Cell Metab* 2012;**15**:764–777.
23. Yoneshiro T, Wang Q, Tajima K, Matsushita M, Maki H, Igarashi K, Dai Z, White PJ, McGarrah RW, Ilkayeva OR, Deleye Y, Oguri Y, Kuroda M, Ikeda K, Li H, Ueno A, Ohishi M, Ishikawa T, Kim K, Chen Y, Sponton CH, Pradhan RN, Majd H, Greiner VJ, Yoneshiro M, Brown Z, Chondronikola M, Takahashi H, Goto T, Kawada T, Sidossis L, Szoka FC, McManus MT, Saito M, Soga T, Kajimura S. BCAA Catabolism in brown fat controls energy homeostasis through SLC25A44. *Nature* 2019;**572**:614–619.
24. Viereck J, Kumarswamy R, Foinquinos A, Xiao K, Avramopoulos P, Kunz M, Dittrich M, Maetzig T, Zimmer K, Remke J, Just A, Fendrich J, Scherf K, Bolesani E, Schambach A, Weidemann F, Zweigerdt R, de Windt LJ, Engelhardt S, Dandekar T, Batkai S, Thum T. Long noncoding RNA chast promotes cardiac remodeling. *Sci Transl Med* 2016;**8**:326ra22.
25. Xu L, Brink M. mTOR, cardiomyocytes and inflammation in cardiac hypertrophy. *Biochim Biophys Acta*. 2016;**1863**:1894–1903.
26. Ruocco C, Ragni M, Rossi F, Carullo P, Ghini V, Piscitelli F, Cutignano A, Manzo E, Ioris RM, Bontems F, Tedesco L, Greco CM, Pino A, Severi I, Liu D, Ceddia RP, Ponzoni L, Tenori L, Rizzetto L, Scholz M, Tuohy K, Bifari F, Di MV, Luchinat C, Carruba MO, Cinti S, Decimo I, Condorelli G, Coppari R, Collins S, Valerio A, Nisoli E. Manipulation of dietary amino acids

prevents and reverses obesity in mice through multiple mechanisms that modulate energy homeostasis. *Diabetes* 2020;**69**:2324–2339.
27. Zhuang L, Jia K, Chen C, Li Z, Zhao J, Hu J, Zhang H, Fan Q, Huang C, Xie H, Lu L, Shen W, Ning G, Wang J, Zhang R, Chen K, Yan X. DYRK1B-STAT3 Drives cardiac hypertrophy and heart failure by impairing mitochondrial bioenergetics. *Circulation* 2022;**145**:829–846.
28. Riehle C, Weatherford ET, Wende AR, Jaishy BP, Seei AW, McCarty NS, Rech M, Shi Q, Reddy GR, Kutschke WJ, Oliveira K, Pires KM, Anderson JC, Diakos NA, Weiss RM, White MF, Drakos SG, Xiang YK, Dale Abel E. Insulin receptor substrates differentially exacerbate insulin-mediated left ventricular remodeling. *JCI Insight* 2020;**5**:134920.
29. Feldman MJ, Russell DH. Polyamine biogenesis in left ventricle of the rat heart after aortic constriction. *Am J Physiol* 1972;**222**:1199–1203.
30. Meana C, Rubín JM, Bordallo C, Suárez L, Bordallo J, Sánchez M. Correlation between endogenous polyamines in human cardiac tissues and clinical parameters in patients with heart failure. *J Cell Mol Med* 2016;**20**:302–312.
31. Huss JM, Imahashi K, Dufour CR, Weinheimer CJ, Courtois M, Kovacs A, Giguère V, Murphy E, Kelly DP. The nuclear receptor ERRα is required for the bioenergetic and functional adaptation to cardiac pressure overload. *Cell Metab* 2007;**6**:25–37.
32. Kamburov A, Cavill R, Ebbels TMD, Herwig R, Keun HC. Integrated pathway-level analysis of transcriptomics and metabolomics data with IMPaLA. *Bioinformatics* 2011;**27**:2917–2918.
33. Sansbury BE, DeMartino AM, Xie Z, Brooks AC, Brainard RE, Watson LJ, DeFilippis AP, Cummins TD, Harbeson MA, Brittian KR, Prabhu SD, Bhatnagar A, Jones SP, Hill BG. Metabolomic analysis of pressure-overloaded and infarcted mouse hearts. *Circ Hear Fail* 2014;**7**:634–642.
34. Davies MN, Kjalarsdottir L, Thompson JW, Dubois LG, Stevens RD, Ilkayeva OR, Brosnan MJ, Rolph TP, Grimsrud PA, Muoio DM. The acetyl group buffering action of carnitine acetyltransferase offsets macronutrient-induced lysine acetylation of mitochondrial proteins. *Cell Rep* 2016;**14**:243–254.
35. Horton JL, Martin OJ, Lai L, Riley NM, Richards AL, Vega RB, Leone TC, Pagliarini DJ, Muoio DM, Bedi KC, Margulies KB, Coon JJ, Kelly DP. Mitochondrial protein hyperacetylation in the failing heart. *JCI Insight* 2016;**1**:e84897.
36. Shirakabe A, Zhai P, Ikeda Y, Saito T, Maejima Y, Hsu CP, Nomura M, Egashira K, Levine B, Sadoshima J. Drp1-dependent mitochondrial autophagy plays a protective role against pressure overload-induced mitochondrial dysfunction and heart failure. *Circulation* 2016;**133**:1249–1263.
37. Bugger H, Schwarzer M, Chen D, Schrepper A, Amorim PA, Schoepe M, Nguyen TD, Mohr FW, Khalimonchuk O, Weimer BC, Doenst T. Proteomic remodelling of mitochondrial oxidative pathways in pressure overload-induced heart failure. *Cardiovasc Res* 2010;**85**:376–384.
38. Shao D, Villet O, Zhang Z, Choi SW, Yan J, Ritterhoff J, Gu H, Djukovic D, Christodoulou D, Kolwicz SC, Raftery D, Tian R. Glucose promotes cell growth by suppressing branched-chain amino acid degradation. *Nat Commun* 2018;**9**:2935.
39. Sun H, Olson KC, Gao C, Prosdocimo DA, Zhou M, Wang Z, Jeyaraj D, Youn JY, Ren S, Liu Y, Rau CD, Shah S, Ilkayeva O, Gui WJ, William NS, Wynn RM, Newgard CB, Cai H, Xiao X, Chuang DT, Schulze PC, Lynch C, Jain MK, Wang Y. Catabolic defect of branched-chain amino acids promotes heart failure. *Circulation* 2016;**133**:2038–2049.
40. Uddin GM, Zhang L, Shah S, Fukushima A, Wagg CS, Gopal K, Al Batran R, Pherwani S, Ho KL, Boisvenue J, Karwi QG, Altamimi T, Wishart DS, Dyck JRB, Ussher JR, Oudit GY, Lopaschuk GD. Impaired branched chain amino acid oxidation contributes to cardiac insulin resistance in heart failure. *Cardiovasc Diabetol* 2019;**18**:86.
41. Sun H, Wang Y. Branched chain amino acid metabolic reprogramming in heart failure. *Biochim Biophys Acta Mol Basis Dis* 2016;**1862**:2270–2275.
42. Shimomura Y, Murakami T, Nakai N, Nagasaki M, Harris RA. Exercise promotes BCAA catabolism: effects of BCAA supplementation on skeletal muscle during exercise. *J Nutr* 2004;**134**:1583S–1587S.
43. Harper AE, Miller RH, Block KP. Branched-chain amino acid metabolism. *Annu Rev Nutr*. 1984;**4**:409–454.
44. Fisch S, Gray S, Heymans S, Haldar SM, Wang B, Pfister O, Cui L, Kumar A, Lin Z, Sen-Banerjee S, Das H, Petersen CA, Mende U, Burleigh BA, Zhu Y, Pinto Y, Liao R, Jain MK. Kruppel-like factor 15 is a regulator of cardiomyocyte hypertrophy. *Proc Natl Acad Sci U S A* 2007;**104**:7074–7079.
45. Wang J, Liu Y, Lian K, Shentu X, Fang J, Shao J, Chen M, Wang Y, Zhou M, Sun H. BCAA Catabolic defect alters glucose metabolism in lean mice. *Front Physiol* 2019;**10**:1140.
46. Ammirati E, Contri R, Coppini R, Cecchi F, Frigerio M, Olivotto I. Pharmacological treatment of hypertrophic cardiomyopathy: current practice and novel perspectives. *Eur J Heart Fail*. 2016;**18**:1106–1118.
47. Zhabyeyev P, Gandhi M, Mori J, Basu R, Kassiri Z, Clanachan A, Lopaschuk GD, Oudit GY. Pressure-overload-induced heart failure induces a selective reduction in glucose oxidation at physiological afterload. *Cardiovasc Res* 2013;**97**:676–685.
48. Butler T. Dietary management of heart failure: room for improvement? *Br J Nutr* 2016;**115**:1202–1217.
49. Chrysohoou C, Pitsavos C, Metallinos G, Antoniou C, Oikonomou E, Kotroyiannis I, Tsantilas A, Tsitsinakis G, Tousoulis D, Panagiotakos DB, Stefanadis C. Cross-sectional relationship of a Mediterranean type diet to diastolic heart function in chronic heart failure patients. *Heart Vessels* 2012;**27**:576–584.
50. Fitõ M, Estruch R, Salas-Salvadõ J, Martínez-Gonzalez MA, Arõs F, Vila J, Corella D, Díaz O, Sáez G, de la Torre R, Mitjavila MT, Muñoz MA, Lamuela-Raventõs RM, Ruiz-Gutierrez V, Fiol M, Gõmez-Gracia E, Lapetra J, Ros E, Serra-Majem L, Covas MI. Effect of the Mediterranean diet on heart failure biomarkers: a randomized sample from the PREDIMED trial. *Eur J Heart Fail* 2014;**16**:543–550.
51. Al-Zaid NS, Dashti HM, Mathew TC, Juggi JS. Low carbohydrate ketogenic diet enhances cardiac tolerance to global ischaemia. *Acta Cardiol* 2007;**62**:381–389.
52. McCommis KS, Kovacs A, Weinheimer CJ, Shew TM, Koves TR, Ilkayeva OR, Kamm DR, Pyles KD, King MT, Veech RL, DeBosch BJ, Muoio DM, Gross RW, Finck BN. Nutritional modulation of heart failure in mitochondrial pyruvate carrier–deficient mice. *Nat Metab* 2020;**2**:1232–1247.
53. Evangelista LS, Jose MM, Sallam H, Serag H, Golovko G, Khanipov K, Hamilton MA, Fonarow GC. High-protein vs. Standard-protein diets in overweight and obese patients with heart failure and diabetes mellitus: findings of the pro-HEART trial. *ESC Hear Fail* 2021;**8**:1342–1348.
54. McGarrah RW, White PJ. Branched-chain amino acids in cardiovascular disease. *Nat Rev Cardiol* 2023;**20**:77–89.
55. Nemutlu E, Zhang S, Xu YZ, Terzic A, Zhong L, Dzeja PD, Cha YM. Cardiac resynchronization therapy induces adaptive metabolic transitions in the metabolomic profile of heart failure. *J Card Fail* 2015;**21**:460–469.
56. Zhang ZY, Marrachelli VG, Yang WY, Trenson S, Huang QF, Wei FF, Thijs L, Van KJ, Monleon D, Verhamme P, Voigt JU, Kuznetsova T, Redón J, Staessen JA. Diastolic left ventricular function in relation to circulating metabolic biomarkers in a population study. *Eur J Prev Cardiol* 2019;**26**:22–32.
57. Felig P, Marliss E, Cahill GF. Plasma amino acid levels and insulin secretion in obesity. *N Engl J Med* 1969;**281**:811–816.
58. Shou J, Chen PJ, Xiao WH. The effects of BCAAs on insulin resistance in athletes. *J Nutr Sci Vitaminol (Tokyo)*. 2019;**65**:383–389.
59. Nagata C, Nakamura K, Wada K, Tsuji M, Tamai Y, Kawachi T. Branched-chain amino acid intake and the risk of diabetes in a Japanese community. *Am J Epidemiol* 2013;**178**:1226–1232.
60. Newgard CB, An J, Bain JR, Muehlbauer MJ, Stevens RD, Lien LF, Haqq AM, Shah SH, Arlotto M, Slentz CA, Rochon J, Gallup D, Ilkayeva O, Wenner BR, Yancy WS, Eisenson H, Musante G, Surwit RS, Millington DS, Butler MD, Svetkey LP. A branched-chain amino acid-related metabolic signature that differentiates obese and lean humans and contributes to insulin resistance. *Cell Metab* 2009;**9**:311–326.
61. Chen S, Miki T, Fukunaga A, Eguchi M, Kochi T, Nanri A, Kabe I, Mizoue T. Associations of serum amino acids with insulin resistance among people with and without overweight or obesity: a prospective study in Japan. *Clin Nutr* 2022;**41**:1827–1833.
62. Nisoli E, Aquilani R, D'Antona G. Amino Acid Supplements and Diabetes. In: Watson R, Preedy VR. Bioactive food as dietary interventions for diabetes. 1st ed. London: Academic Press, 2013:83–95.
63. Shimizu I, Minamino T, Toko H, Okada S, Ikeda H, Yasuda N, Tateno K, Moriya J, Yokoyama M, Nojima A, Koh GY, Akazawa H, Shiojima I, Kahn CR, Abel ED, Komuro I. Excessive cardiac insulin signaling exacerbates systolic dysfunction induced by pressure overload in rodents. *J Clin Invest* 2010;**120**:1506–1514.
64. Tran DH, Wang ZV. Glucose metabolism in cardiac hypertrophy and heart failure. *J Am Heart Assoc* 2019;**8**:e012673.
65. Zhu X, Shen W, Yao K, Wang H, Liu B, Li T, Song L, Diao D, Mao G, Huang P, Li C, Zhang H, Zou Y, Qiu Y, Zhao Y, Wang W, Yang Y, Hu Z, Auwerx J, Loscalzo J, Zhou Y, Ju Z. Fine-Tuning of PGC1α expression regulates cardiac function and longevity. *Circ Res* 2019;**125**:707–719.
66. Piquereau J, Caffin F, Novotova M, Prola A, Garnier A, Mateo P, Fortin D, Huynh LH, Nicolas V, Alavi MV, Brenner C, Ventura-Clapier R, Veksler V, Joubert F. Down-regulation of OPA1 alters mouse mitochondrial morphology, PTP function, and cardiac adaptation to pressure overload. *Cardiovasc Res* 2012;**94**:408–417.
67. Seymour AML, Giles L, Ball V, Miller JJ, Clarke K, Carr CA, Tyler DJ. In vivo assessment of cardiac metabolism and function in the abdominal aortic banding model of compensated cardiac hypertrophy. *Cardiovasc Res* 2015;**106**:249–260.
68. Taegtmeyer H, Young ME, Lopaschuk GD, Abel ED, Brunengraber H, Darley-Usmar V, Des RC, Gerszten R, Glatz JF, Griffin JL, Gropler RJ, Holzhuetter HG, Kizer JR, Lewandowski ED, Malloy CR, Neubauer S, Peterson LR, Portman MA, Recchia FA, Van EJ, Wang TJ. Assessing cardiac metabolism. *Circ Res* 2016;**118**:1659–1701.
69. McMullen JR, Sherwood MC, Tarnavski O, Zhang L, Dorfman AL, Shioi T, Izumo S. Inhibition of mTOR signaling with rapamycin regresses established cardiac hypertrophy induced by pressure overload. *Circulation* 2004;**109**:3050–3055.
70. Shioi T, McMullen JR, Tarnavski O, Converso K, Sherwood MC, Manning WJ, Izumo S. Rapamycin attenuates load-induced cardiac hypertrophy in mice. *Circulation* 2003;**107**:1664–1670.
71. Chen M, Gao C, Yu J, Ren S, Wang M, Wynn RM, Chuang DT, Wang Y, Sun H. Therapeutic effect of targeting branched-chain amino acid catabolic flux in pressure-overload induced heart failure. *J Am Heart Assoc* 2019;**8**:e011625.
72. Sciatti E, Lombardi C, Ravera A, Vizzardi E, Bonadei I, Carubelli V, Gorga E, Metra M. Nutritional deficiency in patients with heart failure. *Nutrients*. 2016;**8**:442.
73. Carubelli V, Castrini AI, Lazzarini V, Gheorghiade M, Metra M, Lombardi C. Amino acids and derivatives, a new treatment of chronic heart failure? *Heart Fail Rev* 2015;**20**:39–51.

Translational perspective

Recent studies have identified the critical role of amino acid metabolism perturbation in the pathogenesis of heart failure with reduced ejection fraction. The consumption of a designer diet, in which a specifically formulated free essential amino acid mixture substitutes for proteins, improves branched-chain amino acid oxidation and attenuates systolic dysfunction in transverse aortic constriction-induced left ventricle pressure overload in mice. In addition, the substituted diet increases energy metabolism, promoting myocardial bioenergetics, efficient substrate utilization, and reduces fibrosis. The dietary modulation of energy production and amino acid metabolism represents a novel therapeutic paradigm to prevent or treat cardiac dysfunction, a promising supportive approach for treating cardiac diseases with depressed cardiac ejection fraction.